

1986

Peroxo Complexes of Molybdenum (VI) and Vanadium (V) with Imidazole and Histidine

Jennifer Lisa Gundersen

College of William & Mary - Arts & Sciences

Follow this and additional works at: <https://scholarworks.wm.edu/etd>

 Part of the [Inorganic Chemistry Commons](#), and the [Organic Chemistry Commons](#)

Recommended Citation

Gundersen, Jennifer Lisa, "Peroxo Complexes of Molybdenum (VI) and Vanadium (V) with Imidazole and Histidine" (1986). *Dissertations, Theses, and Masters Projects*. Paper 1539625344.

<https://dx.doi.org/doi:10.21220/s2-0s1q-jw81>

This Thesis is brought to you for free and open access by the Theses, Dissertations, & Master Projects at W&M ScholarWorks. It has been accepted for inclusion in Dissertations, Theses, and Masters Projects by an authorized administrator of W&M ScholarWorks. For more information, please contact scholarworks@wm.edu.

PEROXO COMPLEXES OF MOLYBDENUM(VI) AND
VANADIUM(V) WITH IMIDAZOLE AND HISTIDINE

A Thesis

Presented to

The Faculty of the Department of Chemistry
The College of William and Mary in Virginia

In Partial Fulfillment

Of the Requirements for the Degree of
Master of Arts

by

Jennifer Lisa Gundersen

1986

APPROVAL SHEET

This thesis is submitted in partial fulfillment of
The requirements for the degree of

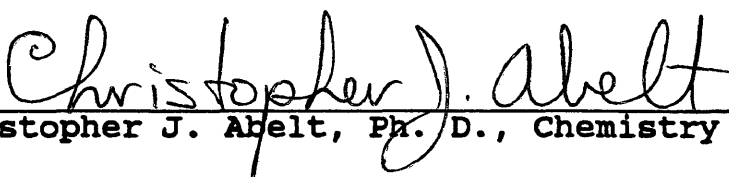
Master of Arts


Author

Approved, June 1986


Cirila Djordjevic, Ph. D., Chemistry


David W. Thompson, Ph. D., Chemistry


Christopher J. Abelt, Ph. D., Chemistry

Dedication

This paper is dedicated to my mother, Florence Gundersen, and to the memory of my grandfather, Josef Dombrowski, for their true appreciation of the value of an education.

Table of Contents

	Page
Acknowledgements.....	vi
List of Tables.....	vii
List of Figures.....	viii
Abstract.....	x
1. Introduction.....	2
2. Review of Literature.....	4
2.1 Chemistry of Vanadium.....	4
2.2 Chemistry of Molybdenum.....	15
2.3 Metal Complexes with Imidazole.....	35
2.4 Metal Complexes with Histidine.....	50
3. Results and Discussion.....	59
3.1 Peroxo imidazole vanadates.....	59
3.2 Peroxo imidazole molybdates.....	61
3.3 Peroxo oxalato molybdates.....	78
3.4 Peroxo histidine molybdates.....	85
4. Experimental.....	92
4.1 Preparation of the Compounds.....	92
4.1.1 Vanadium-imidazole system.....	92
4.1.1.1 System $K/V/O/O_2/im$	92
4.1.1.2 System $V/O/O_2/im$	94
4.1.2 Molybdenum-imidazole system.....	97
4.1.2.1 System $K/Mo/O/im$	97
4.1.2.2 $MoO(O)_2 \cdot im \cdot H_2O$	98
4.1.2.3 $MoO(O)_2 \cdot im \cdot H_2O$	99

4.1.2.4	System $\text{NH}_4/\text{Mo}/\text{O}/\text{O}_2/\text{im}$	100
4.1.2.5	System $\text{K}/\text{Mo}/\text{O}/\text{O}_2/\text{im}$	101
4.1.3	Molybdenum-imidazole-aspartate system...	102
4.1.3.1	$\text{K}_2[\text{MoO}(\text{O}_2)_2(\text{C}_2\text{O}_4)]$	102
4.1.4	Molybdenum-aspartate system.....	104
4.1.4.1	$\text{K}_2[\text{MoO}(\text{O}_2)_2(\text{C}_2\text{O}_4)]$	104
4.1.5	Molybdenum-histidine system.....	105
4.1.5.1	System $\text{Mo}/\text{O}/\text{O}_2/\text{his}$	105
4.1.5.2	System $\text{NH}_4/\text{Mo}/\text{O}/\text{O}_2/\text{his}$	106
4.1.5.3	System $\text{K}/\text{Mo}/\text{O}/\text{O}_2/\text{his}$	108
4.2	Physical measurement of the compounds.....	109
4.2.1	Infrared spectra.....	109
4.2.1.1	Nujol mulls.....	109
4.2.1.2	HCBD mulls.....	109
4.2.2	UV/visible spectra.....	110
4.3	Analysis of the complexes.....	111
4.3.1	Analysis for peroxide.....	111
4.3.1.1	Ce(IV) titration.....	111
4.3.2	C, H, N analysis.....	112
4.3.3	Molybdenum analysis.....	112
4.3.4	X-ray structure analysis.....	112
5.	Conclusion.....	113
	References.....	115

Acknowledgements

The author would like to express her sincere appreciation to Professor Cirila Djordjevic, under whose guidance this research was conducted, for her support and encouragement throughout this project. The author would also like to thank Professors Christopher J. Abelt and David W. Thompson for their careful reading of this manuscript. Special thanks must also be given to Irene Molyneux, Geraldine Murphy, Glenn Gundersen and Susan Manix for their support when the going got tough.

Funding for this project was provided by the National Science Foundation.

List of Tables

	Page
1. Oxidation states and Coordination of Vanadium.....	7
2. Reactions of V(V) in aqueous media.....	8
3. Peroxo complexes with Vanadium.....	14
4. Oxidation states and Coordination of Molybdenum.....	33
5. Peroxo complexes with Mo(VI).....	34
6. Metal complexes with Imidazole.....	49
7. C, H, N and peroxide analysis of complexes and systems.....	91

List of Figures

	Page
1. Species of Vanadium in solution.....	12
2. Coordination of metal-peroxo complexes.....	13
3. Formulae for metal-peroxo complexes.....	13
4. Structure of $\text{Mo}_6\text{X}^{+4}_8$ cluster compound.....	24
5. Structure of $(\eta^5\text{-C}_5\text{H}_5)_2\text{MoCl}_2$	25
6. Histidine.....	26
7. Structure of $\{[\text{Mo(V)O}_2(\text{C}_2\text{O}_4)(\text{H}_2\text{O})]_2\text{O}_2\}^{-2}$	27
8. Structure of $\{[\text{Mo(VI)O}_2(\text{C}_2\text{O}_4)(\text{H}_2\text{O})]_2\text{O}\}^{-2}$	28
9. Structure of $\text{Mo(VI)O}_2(\text{acac})_2$	29
10. Structure of $[\text{Mo(VI)O}(\text{O}_2)_2(\text{C}_2\text{O}_4)]^{-2}$ anion.....	30
11. Distorted pentagonal bipyramid.....	31
12. Structures of $\text{MoO}(\text{O}_2)_2\text{gly.H}_2\text{O}$ and $\text{MoO}(\text{O}_2)_2\text{pro.H}_2\text{O}$	32
13. Imidazole.....	37
14. Pyrrole.....	37
15. Pyridine.....	37
16. Imidazole cation.....	44
17. Imidazole anion and metal bridge.....	44
18. Species of imidazole in solution.....	45
19. Structure of $\text{Cu}(\text{im})_4\text{I}_2$	46
20. Structure of $\text{Zn}(\text{im})_2$ and $\text{Cu}(\text{im})_2$ polymers.....	47
21. Structure of $\text{Cu}(\text{im})_2$ polymer.....	48
22. Species of histidine in solution.....	54

23. Metal complexes with histidine.....	55
24. Co(II)-histidine complexes.....	56
25. Coordination of Pt(II)-histidine complex.....	57
26. Structure of $\text{Mo(V)}_2\text{O}_4(\text{L-his})_2$	58
27. Possible structure of $\text{MoO}(\text{O}_2)_2 \text{ im.H}_2\text{O}$	70
28. IR of imidazole.....	71
29. IR of $\text{MoO}(\text{O}_2)_2 \text{ im.H}_2\text{O}$	72
30. UV/visible spectra.....	73
31. Possible structure of $\text{MoO}_2(\text{O}_2)_2 \text{ im.H}_2\text{O}$	74
32. IR of $\text{MoO}_2(\text{O}_2) \text{ im.H}_2\text{O}$	75
33. IR of $\text{K/Mo/O/O}_2/\text{im}$	76
34. IR of K/Mo/O/im	77
35. Malic, malonic, succinic and aspartic acid.....	82
36. IR of $\text{K}_2[\text{MoO}(\text{O}_2)_2(\text{C}_2\text{O}_4)]$	83
37. Sample Ce(IV) titration curves.....	84
38. IR of histidine.....	89
39. IR of $\text{K/Mo/O/O}_2/\text{his}$	90

Abstract

Imidazole and histidine are important molecules, involved in bonding with metal ions in living matter and investigated in a number of model systems in biochemistry. We have investigated Mo(VI) and V(V) peroxo systems with imidazole and histidine and have prepared the first peroxo-imidazole ligand combinations observed so far. Crystalline complexes with the formulae $\text{MoO}(\text{O}_2)_2 \cdot \text{im.H}_2\text{O}$ and $\text{MoO}_2(\text{O}_2) \cdot \text{im.H}_2\text{O}$, both stable compounds, were obtained. In addition, the conversion of aspartate to oxalate by the aqueous Mo(VI)-peroxo system, resulting in the formation of the known compound $\text{K}_2[\text{MoO}(\text{O}_2)_2(\text{C}_2\text{O}_4)]$, was observed.

Both imidazole complexes are soluble in water. For $\text{MoO}(\text{O}_2)_2 \cdot \text{im.H}_2\text{O}$ the peroxo----> metal charge transfer occurs at 315 nm. For $\text{MoO}_2(\text{O}_2) \cdot \text{im.H}_2\text{O}$ the charge transfer occurs at 320 nm at pH 1. The IR spectrum of the diperoxo complex reveals distinct bands at 960 cm^{-1} and 860 cm^{-1} for the Mo=O and O-O stretching modes, respectively. The analogous vibrations for the monoperoxo species occur at 950 cm^{-1} and 850 cm^{-1} . The isolation of $\text{MoO}(\text{O}_2)_2 \cdot \text{im.H}_2\text{O}$ in the form of crystals large enough for x-ray analysis was accomplished and x-ray structure analysis of this compound is in progress.

Attempts to obtain peroxo complexes with histidine have not yet been successful. Further investigations are in progress.

**PEROXO COMPLEXES OF MOLYBDENUM(VI) AND
VANADIUM(V) WITH IMIDAZOLE AND HISTIDINE**

Introduction

Mo(VI) and V(V) peroxo complexes are currently of great interest. They are very well known as industrial catalysts and are probably just as important in biochemical systems. Molybdenum and vanadium have been determined to be essential for life and serve as cofactors for many enzymes and proteins. These synthetic peroxo complexes may serve as models for the activity of vanadium and molybdenum in living systems.

Imidazole and histidine are also of great biological significance. They function in several metalloprotein systems and in the iron-heme system of hemoglobin and myoglobin. They serve as ligands to many transition metals in biochemical systems.

We have, therefore, attempted to synthesize heteroligand peroxo metal complexes of Mo(VI) or V(V) with either histidine or imidazole. Crystalline complexes were separated from the Mo-imidazole system and are currently under further study. The effect of another ligand in this system (aspartic acid) was then studied with the hope of obtaining a Mo peroxo complex containing both imidazole and aspartate. Instead the aspartic acid was converted to oxalate by the aqueous Mo system yielding a known complex, $K_2[MoO(O_2)_2(C_2O_4)]$.

This thesis reviews the coordination chemistry and

biological significance of molybdenum and vanadium as well as the transition metal complexes of imidazole and histidine. The results of our experimental work are analyzed and discussed and the experimental procedures are described in the third and fourth chapters.

2 Review of Literature

2.1 The Chemistry of Vanadium

Recent studies have shown that vanadium is not only present in plant and animal tissues but that it is an essential element in these systems. <1,2> In the earth's crust it is present at a level of about 135 ppm, while plants contain an average of 1-2 ppm and animals usually contain less than 1 ppm.<1> Some plants, such as the highly toxic<3> mushroom, *Amanita muscaria*, are known to concentrate vanadium and can contain up to 100 times the average. A number of animals are also vanadium concentrators. Many marine animals in the class Ascidiaceae have exhibited concentrations that are hundreds of times the mean concentration<1>.

Studies have indicated that vanadium is an essential trace metal for humans and other animals but its function is not precisely known yet. Though it is essential, intake levels that are not much higher than necessary have shown toxic effects including disturbances of the nervous system and breathing difficulties. Severe overdoses can cause death <4>. The effects of vanadium deficiency are currently under study and have not been well defined yet <5>.

The inorganic and coordination chemistry of vanadium has been known and studied much longer and therefore has a much larger body of information behind it. Vanadium exists in oxidation states ranging from -1 to +5 with the +4 and +5 states being the most stable <6>. The oxidation states +3, +4 and +5 are known to exist in biological systems but the +3 state is quite rare <2>. The coordination and geometry of the various states is given in Table 1.

Vanadium forms several oxides including V_2O_3 , VO , V_2O_5 , V_5O_9 and VO_2 as well as those with non-stoichiometric formulae. V_2O_5 is the most stable and common oxide of the metal. It is the final step in the oxidation of vanadium metal <7>. V_2O_5 dissolves readily in basic media and, although it is an acidic compound, it also dissolves in acids. The species that is present in an aqueous medium depends greatly on the pH and the concentration of the vanadium in solution. This dependence is exhibited in figure 1. On dissolving V_2O_5 in a base, such as NaOH, a colorless solution is obtained. With addition of acid, the solution remains colorless until a pH of 6.5 is attained. The solution then turns orange. When a pH of 2 is reached V_2O_5 will precipitate out but it redissolves as pH 0 is approached. VO_2^+ is then formed <6>.

In highly basic, aqueous solutions the species VO_4^{3-} is a monomer but it hydrolyses rapidly to HVO_4^{2-} ($[VO_3(OH)]^{-2}$). As the pH drops the monomer condenses to the dimer, $V_2O_7^{4-}$.

then to the trimer, $V_3O_9^{-3}$ <7>. These and the remaining equilibrium reactions are given in Table 2.

Table 1
Oxidation States and Stereochemistry of Vanadium

ref. 6

Oxidation state	Coordination number	Geometry	Examples
V ⁻¹	6	Octahedral	V(CO) ₆ ⁻ , Li[V(bipy) ₃]·4C ₆ H ₆ O
V ⁰	6	Octahedral	V(CO) ₆ , V(bipy) ₃ , V[C ₂ H ₄ (PMe ₂) ₂] ₃
	7	?	V(CO) ₆ AuPPh ₃
V ^I , d ⁴	6	Octahedral	[V(bipy) ₃] ⁺
		Tetragonal pyramidal	k ² -C ₂ H ₅ V(CO) ₄
V ^{II} , d ³	6	Octahedral	[V(H ₂ O) ₆] ²⁺ , [V(CN) ₆] ³⁻
V ^{III} , d ²	3	Planar	V[N(SiMe ₃) ₂] ₃
	4	Tetrahedral	[VC ₄] ⁻
	5	<i>trp</i>	<i>trans</i> -VC ₃ (SMe ₂) ₂ , VC ₃ (NMe ₂) ₂
	6 ^a	Octahedral	[V(NH ₃) ₆] ³⁺ , [V(C ₂ O ₄) ₃] ³⁻ , VF ₃
V ^{IV} , d ¹	4	Tetrahedral	VC ₄ , V(NEt ₂) ₄ , V(CH ₂ SiMe ₃) ₄
	5	Tetragonal pyramidal	VO(acac) ₂
		?	[VO(SCN) ₄] ³⁻ , VC ₅
		<i>trp</i>	VOC ₂ <i>trans</i> -(NMe ₂) ₂
	6 ^a	Octahedral	VO ₂ (rutile), K ₂ VC ₆ , VO(acac) ₂ py
	8	Dodecahedral	VC ₈ (diars) ₂
V ^V , d ⁰	4	Tetrahedral(C _{3v})	VOC ₃
	5	<i>trp</i>	VF ₅ (g)
		<i>spy</i>	C ₂ VOF ₄
	6 ^a	Octahedral	VF ₅ (s), VF ₆ , V ₂ O ₅ (very distorted, almost <i>trp</i> with one distant O); [VO ₂ ox ₂] ³⁻
	7	Pentagonal bipyramidal	VO(NO ₂) ₃ ·CH ₃ CN ^b

^a Most important states.

^b Contains both mono- and bi-dentate NO₂ groups (F. B. W. Einstein *et al.*, *Inorg. Chem.*, 1971, 10, 678).

Table 2
Reactions of V(V) in aqueous solutions

refs. 6,7

Reaction	-log K
(in basic media)	
$\text{HVO}_4^{-2} \rightleftharpoons \text{H}^+ + \text{VO}_4^{-3}$	13.0 + 0.3
$\text{VO}_4^{-3} + \text{H}_2\text{O} \rightleftharpoons \text{HVO}_4^{-2} + \text{OH}^-$	1.01 + 0.02
$2\text{HVO}_4^{-2} \rightleftharpoons \text{V}_2\text{O}_7^{-4} + \text{H}_2\text{O}$	-1.68 + 0.04
$2\text{HVO}_4^{-2} + \text{H}_2\text{O} \rightleftharpoons \text{HV}_2\text{O}_7^{-3} + \text{OH}^-$	3.18 + 0.05
$\text{HVO}_4^{-2} + \text{H}_2\text{O} \rightleftharpoons \text{H}_2\text{VO}_4^{-} + \text{OH}^-$	5.89 + 0.06
$\text{H}_2\text{VO}_4^{-} \rightleftharpoons \text{H}^+ + \text{HVO}_4^{-2}$	7.88
(in acidic media)	
$\text{H}_3\text{VO}_4 \rightleftharpoons \text{H}_2\text{VO}_4^{-} + \text{H}^+$	3.40
$\text{VO}_2^+ + \text{H}_2\text{O} \rightleftharpoons \text{HVO}_3 + \text{H}^+$	3.30
$10\text{VO}_2^+ + 8\text{H}_2\text{O} \rightleftharpoons \text{H}_2\text{V}_{10}\text{O}_{28}^{-4} + 14\text{H}^+$	6.75 + 0.15
$\text{H}_2\text{V}_{10}\text{O}_{28}^{-4} \rightleftharpoons \text{HV}_{10}\text{O}_{28}^{-5} + \text{H}^+$	4.34
$\text{HV}_{10}\text{O}_{28}^{-5} \rightleftharpoons \text{V}_{10}\text{O}_{28}^{-6} + \text{H}^+$	6.94

There is still some doubt about the existence of some of the species mentioned in Table 2 and figure 1. The Rossottis proposed the existence of $V_{10}O_{28}^{-6}$ in 1956 <8,9> but subsequent studies <10> gave no evidence for such an ion.

Spectral studies indicate that the VO_4^{-3} ion is a tetrahedral. The structures of the dimer and trimer are also based on this structure but the the structure of the decavanadate ions; $V_{10}O_{28}^{-6}$, $HV_{10}O_{28}^{-5}$ and $H_2V_{10}O_{28}^{-4}$ is still unresolved <7>.

No V(V)-imidazole complexes have been reported yet though complexes with the oxovanadium(IV) ion, VO , and both histidine and imidazole have been synthesized. The imidazole complex, in a frozen aqueous medium, has the formula $[VO(im)_4]^{+2}$ with all four imidazoles oriented in the same manner and equivalent <11>.

Peroxo complexes of vanadium are of great interest for several reasons. They are well known as catalysts<12> and may well be a model system for the biochemistry of vanadium <13>. Some complexes have shown antitumor activity against murine L1210 leukemia. The effectiveness of the complex seems to depend on the type of heteroligand species in the compound <14>.

Vanadium peroxo complexes can exist with one, two or three peroxo groups per vanadium atom. In aqueous media the number of peroxy groups per atom increases with

increasing alkalinity. When the acidity increases the degree of polymerization increases as the number of peroxo groups per atom decreases. The degree of polymerization will decrease with increasing hydrogen peroxide concentration <7>.

As seen in figure 1, V(V) exists as VO_2^+ in acidic media. On addition of hydrogen peroxide two distinct species can form: the red monoperoxy vanadate or the yellow diperoxy vanadate <15,16>. The equilibrium reactions are given below:



A high H_2O_2 concentration and low hydrogen ion concentration (high pH) tend to favor the formation of the diperoxo species. It is stable in solution at $\text{pH} > 7$ <17>. Acidifying the solution will convert the yellow diperoxo vanadate back to the red monoperoxy species <15>. Further addition of hydrogen peroxide in an alkaline solution will convert the diperoxospecies to a blue triperoxo species. Deep blue, crystalline complexes of the formula $\text{A}_2[\text{V}(\text{O}_2)_3\text{F}]$, ($\text{A} = \text{NH}_4$, Na or K), have been isolated and characterized <17>. Infrared spectral studies have shown that the oxo group on the diperoxo species probably abstracts an oxygen from the hydrogen peroxide and is converted to the third peroxo group <17>.

There are several ways that a peroxy group can bind to one or two transition metals. These are illustrated in figure 2 and their formulae are listed in figure 3 <18>. As seen in figure 2 peroxide can be bridging or terminal, monodentate or bidentate. As a bridging ligand it can be cis or trans-planar or trans non-planar. The monodentate forms are very unstable. The bidentate, triangular coordination is quite common and stable <17>.

Several very interesting peroxo complexes of V(V) have already been synthesized and characterized. They are summarized in Table 3.

The complexes all contain one to three peroxo groups as well as one or more inorganic or organic ligands that are mono or bidentate. These other ligands can help to stabilize the complex and can also affect the reactivity of the peroxo groups <24>. The peroxo groups can also have a similar effect by stabilizing the heteroligand sphere. This could lead to the formation of a complex that normally would not form without the peroxide <25>. It has been determined that the pH, metal and heteroligand concentrations all have a great effect on the complexing behavior of these complexes <24>.

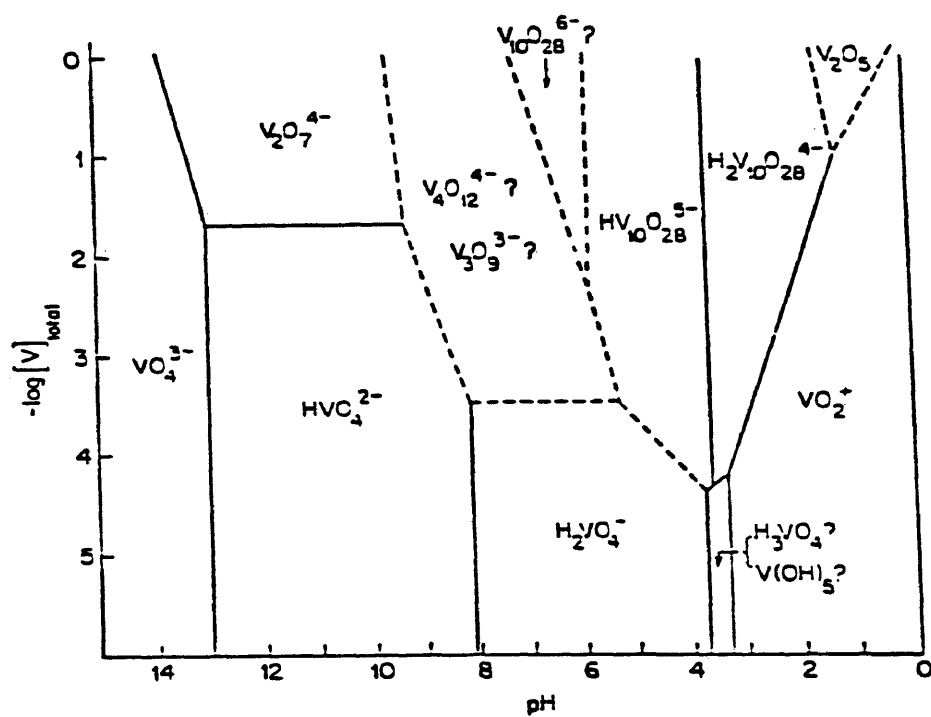


Figure 1. Species of vanadium present in aqueous solution at various concentrations and pH values.

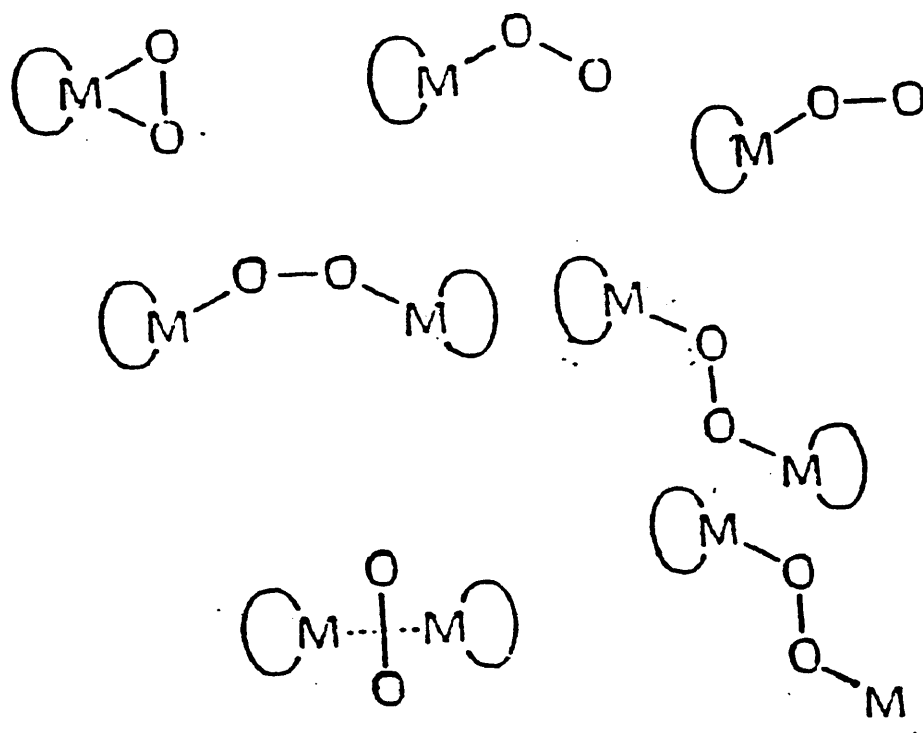


Figure 2. Ways in which the peroxo group may coordinate to a transition metal

- (a) $[M(O_2)_x L_y]^{n-}$
- (b) $[MO_x(O_2)_y L_z]^{m-}$
- (c) μ -oxo
- (d) μ -peroxo

$L = F, Cl, NH_3, C_2O_4, NTA, EDTA,$
dipy, c-phen, oxine, porphyrin,
pyridine-2,6-dicarboxylate.

Figure 3. Formulae of Transition metal peroxo complexes.

Table 3
Peroxo complexes with Vanadium(V)

Compound	Reference
$A[VO(O_2)_2 L] \cdot nH_2O$ (A=Na, K, H or NH_4 ; L= bipyridyl or phenanthroline)	19
$M_3[VO(O_2)_2 (C_2O_4)] \cdot 2H_2O$ (M=K or NH_4)	19
$M_3[V_2O_2(O_2)_4 F] \cdot nH_2O$ (M=K or NH_4 ; n=2)	20
$M_3[HV_2O_2(O_2)_3 F_4] \cdot 2H_2O$ (M=K or NH_4)	20
$M_2[V(O_2)_3 F]$ (M=K, NH_4 or K)	17
$M[VO(O_2)IDA]$ (M=K or NH_4 ; IDA= $[C_4H_7NO_4]$)	13
$Na_3[VO(O_2)EDTA] \cdot 4H_2O$	21
$Na[VO(O_2)H_2EDTA] \cdot 4H_2O$	22
$H[VO(O_2)(dipic)H_2O] \cdot H_2O$ (dipic=dipicolinic acid)	23
$A_2[VO(O_2)NTA]$ (A=K, Na, NH_4 , Rb, Cs, Ca/2, Sr/2, Ba/2)	TBP*

* - to be published- C. Djordjevic et. al.

2.2 The Chemistry of Molybdenum

Molybdenum is a cofactor in many important enzymes such as nitrate reductase, xanthine oxidase, aldehyde oxidase <26>, xanthine dehydrogenase and sulfite oxidase <27,28>. It is an essential trace metal in plants, animals and microorganisms <26,27,29>. Its biological function is much more well known than that of vanadium. About 9.3 mg of Mo is present in the average human with the greatest concentrations in the liver (~2 mg) and kidneys. In the earth's crust and in plants it is present at a concentration of ~1 ppm <4>.

The effect of molybdenum deficiency has been well documented. Studies have shown retarded growth rates and high infant mortality rates in Mo deficient goats. The metabolism of copper is also affected by molybdenum deficiencies <30>. Exposure to excessive amounts of MoO_3 dust has been found to be very toxic to rabbits- irritating the eyes and respiratory tract <4>. Ingesting excessive amounts of molybdenum causes the depletion of copper and may be involved in a disease of the central nervous system called Wilson's disease <29>. The excessive intake of Mo is often said to have an antagonistic effect on the metabolism of copper <31>.

Much of the chemistry of molybdenum revolves around understanding its function in enzymes and living

systems in general. To that end many inorganic chemists are attempting to synthesize molybdenum complexes that could mimick the the role of this metal in certain enzymes<27>.

Molybdenum can exist in oxidation states ranging from -II to +VI (excluding -I). Its chemistry often parallels that of chromium and tungsten. Some examples of Mo compounds along with their geometry are listed in Table 4. The lower oxidation states (-II, 0, I) are dominated by by compounds with π -acceptor ligands such as $\text{Mo}(\text{CO})_6$. One or more of the CO groups can be substituted for many other ligands such as NO, CN, NH_4 or halogens<29>. Organometallic complexes are also characteristic of these oxidation states. These complexes include $(\text{C}_6\text{H}_6)_2\text{Mo}$ <32>, $\pi\text{-C}_5\text{H}_5\text{-Mo}(\text{CO})_3\text{H}$ <33> and $\sigma\text{-CH}_3\text{Mo}(\text{CO})_3(\pi\text{-C}_5\text{H}_5)$ <34>.

The distinction between these organometallic complexes and the π -acceptor complexes is that at least one of the organic ligands in the organometallic compound is bonded to the metal by its π -electron system and the ligand itself lies at a 90 degree angle to the bond. The π -acceptor ligands lie in the plane of the bond<29>.

The chemistry of the +II oxidation state is described almost entirely by halogen compounds and derivatives, though some organometallic compounds are also known<27>. In this oxidation state metal-metal bonds and cluster compounds form readily<29>. The clusters have the general

formula $\text{Mo}_6\text{X}_8^{+4}$. (X= halogen). Its basic structure is shown in figure 4. In MoCl_2 , the $\text{Mo}_6\text{Cl}_8^{+4}$ units are connected by four bridging chlorines with two additional non-bridging chlorines in the remaining positions<35>.

Mo(III) is not known for many coordination compounds though thousands of Cr(II) complexes are known. Several trihalide compounds and derivatives (dimers and trimers) have been prepared<27>. Complexes with CN , isothiocyanide(NCS), acetylacetone and hydroxide as well as Mo_2O_3 have been reported<29>.

Mo(IV) is characterized by halides as well as chelate and coordination compounds. The halide compounds are quite unstable and will disproportionate when heated. For example, heating MoCl_4 to 170 C yields MoCl_5 and MoCl_3 . In vacuo at 150 C MoCl_3 and Cl_2 is obtained <29>.

Mo(IV) halides can also form adducts with organic ligands giving hexacoordinate species of the form $\text{MoX}_4 \cdot 2\text{L}$ or $\text{MoX}_4 \cdot \text{B}$ (L=monodentate ligands, B=bidentate ligands). Several cyanide complexes are also known-ranging from the dodecahedral $[\text{Mo}(\text{CN})_8]^{+3}$ ion to to the octahedral $\text{K}_3[\text{MoO}_2(\text{CN})_4] \cdot 6\text{H}_2\text{O}$ <29>. Many complexes with C_5H_5 have also been reported. The cyclopentadienyl group tends to coordinate through its π -system as in the Mo(III) complexes. The structure of $(\eta\text{-C}_5\text{H}_5)\text{MoCl}_2$ is given in figure 5 <27>.

The oxidation states +V and +VI are, by far, the most

stable and studied oxidation states. Mo(V) forms the usual halide compounds with the formula MoX_5 as well as complex halide and oxyhalide compounds of the general formulae $\text{M}[\text{MoX}_6]$ and MoOX_3 . The oxyhalide reacts with many different organic ligands to form adducts with the formulae MoOCl_3L and MoOCl_3B . Mo(V) also forms more complex and chelate compounds than the previously mentioned states<29>.

Histidine complexes with both Mo(V) and Mo(VI) have been reported. The Mo(V)-his complex forms in a ratio of 1:1 in slightly acidic solutions. It is far less stable than the Mo(VI) complex which forms in the pH range of 4.8 to 8.0. The Mo-his ratio is 1:1 at pH 6.0 and increases with lower pH values<36>. No e.p.r signal was observed with the Mo(V) complex. This means that there are no paramagnetic species present and the species is, therefore, probably dimeric<29>. The Mo(VI) complex is apparently monomeric with the histidine coordinating through the amino group and the number 1 nitrogen on the imidazole ring. See figure 6 <36>.

Mo(V) forms an interesting complex with oxalate. The complex, $\text{Ba}[\text{Mo}_2\text{O}_4(\text{C}_2\text{O}_4)_2] \cdot 5\text{H}_2\text{O}$ is binuclear. The two Mo(V) atoms are hexacoordinated in a distorted octahedral and are joined by two bridging oxygens. The anion of the salt is shown in figure 7 <29,37>. Other ligands that form chelate compounds or complexes with Mo(V) are EDTA, PDTA, MIDA, NTA and acetonitrile <29>.

For Mo(VI) there is only one reported simple halide, MoF_6 (m.p. 17°C). In the vapor phase (b.p. 35°C) it is monomeric with the point group C_h . At room temperature its symmetry is greatly decreased<29>. The oxyhalides exist in two forms- MoO_2X_2 (X=F, Cl, Br) and MoOX_4 (X=F, Cl). In the vapor phase they are monomeric but they tend to polymerize in the liquid and solid phase<29>.

Several chelate and complex compounds have also been synthesized. Besides the Mo(VI)-his complex already discussed, two oxalato complexes have been reported. The first complex, $\text{K}_2[\text{MoO}_2(\text{C}_2\text{O}_4)_2(\text{H}_2\text{O})_2]\cdot 2\text{H}_2\text{O}$, is binuclear with a single, linear Mo-O-Mo bridge<38>. The other complex, $\text{NaNH}_4[\text{MoO}_3(\text{C}_2\text{O}_4)]\cdot 2\text{H}_2\text{O}$, is polymeric with bent and distorted Mo-O-Mo-O linkages. The structure of the first complex is shown in figure 8 <39>. Several other complexes of the form MoO_2L_2 (L=b-diketonate) have been prepared. NMR spectral studies have indicated that the two oxo groups are in a cis configuration as seen in the structure of $\text{MoO}_2(\text{acac})_2$ in figure 9 <27>.

Of growing importance is the field of Mo(VI)-peroxo complexes. Peroxo complexes only form with the metal in the +6 oxidation state<40>. Numerous Mo(VI)-peroxo complexes have already been reported with peroxo to metal ratios of 4:1, 3:1, 2:1, 1:1 and ratios of less than 1:1<40>.

Peroxide complexes of transition metals are usually

very unstable. They can explode spontaneously when heated or struck. Others are quite stable to heating or exposure to the atmosphere and remain unchanged for years in closed containers<18>.

The tetraperoxo species has the formula $\text{Mo}(\text{O}_2)_4^{-2}$. Red salts have been isolated with the cations Na^+ , K^+ , Ca^+ , Sr^+ , Ba^+ , Co^+ , and $\text{Zn}(\text{NH}_4)^+ 2$. It is not known whether all four of the peroxo groups are directly bound to the metal atom or not. Some substances may contain an H_2O_2 of crystallization. Most of the complexes are quite unstable. $\text{K}_2[\text{Mo}(\text{O}_2)_4]$ is deep red in aqueous solution but it slowly changes to yellow, accompanied by an evolution of oxygen. If an excess of H_2O_2 is present in alkaline solution, the ion remains more stable. The proposed equilibrium between these two species is given below:



The triperoxo species are given the formula $\text{MoO}(\text{O}_2)_3^{-2}$ and are generally unstable at room temperature. At present there is some uncertainty surrounding the actual existence of this species. It has been postulated that the solids that seem to exhibit this formula are actually a mixture of the tetraperoxo and diperoxo species. Other theories suggest that the dimeric salt shown above has two hydrogen peroxides of crystallization<40>.

The 2:1 species, $\text{MoO}_2(\text{C}_2\text{O}_4)_2^{-2}$, is more stable than the tetraperoxo species. It generally exists as the dimer mentioned above. Thermal decomposition of this species yields a molybdate $(\text{MoO}_4)^{-2}$. There is a possibility that a monoperoxo species is an intermediate in this decomposition<29>.

Several salts of the 1:1 species have been synthesized with the formula $\{(\text{M}_2, \text{M} \text{ or } \text{H}_2)[\text{MoO}_3(\text{O}_2)] \cdot x\text{H}_2\text{O}\}$. Many studies have cast doubts on the existence of such a species in solution though crystalline products have been obtained. A report by E.J. Richardson in 1960 indicated that the species is polymeric in solution<41>.

Many complexes have been isolated that have between 0 and 1 peroxide group per Mo atom such as $\text{Ba}_5\text{Mo}_{12}\text{O}_{38}(\text{O}_2)_3 \cdot 18\text{H}_2\text{O}$. There is very little recent literature on these types of complexes and their structures have not yet been elucidated<40>.

Several Mo(VI)-peroxo complexes of varying forms are summarized in Table 5. Some of the more interesting compounds are discussed below.

$\text{K}_2[\text{MoO}(\text{O}_2)_2(\text{C}_2\text{O}_4)]$ (figure 10) was originally prepared by dissolving oxalatomolybdates in H_2O_2 at 0°C<42>. A new catalysis has recently been reported where malonic acid and malic acid were converted to oxalate in aqueous peroxomolybdate(VI) solutions resulting in the formation of the same pentagonal bipyrimidal complex<43>. A similar

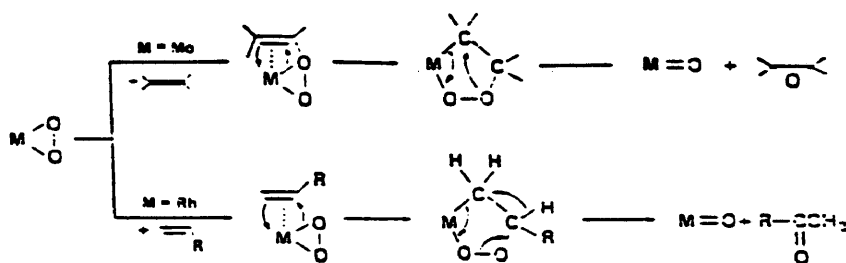
catalysis involving the conversion of aspartic acid to oxalate and subsequently $K_2[MoO(O_2)_2(C_2O_4)]$ is reported in this paper and will be discussed further later (see section 3.3).

Many of the mono and diperoxo complexes listed in Table 5 including $MoO(O_2)(dipic) \cdot H_2O$ and $MoO(O_2)_2 \text{glycine} \cdot H_2O$ exhibit the distorted pentagonal bipyramid structure. This is a very common geometry for molybdenum.

Peroxo complexes with α -amino acids are currently under study. Complexes of the form $MoO(O_2)_2(\alpha-AA)$ have been synthesized for the amino acids: glycine, proline, leucine, serine, alanine and valine<44>. Their biochemical significance is currently being examined. Figures 11 and 12 show the typical distorted pentagonal bipyramidal coordination of Mo(VI)-peroxo complexes as well as some representative crystal structures for complexes of the formula: $MoO(O_2)_2(\alpha-AA) \cdot H_2O$.

While molybdenum peroxides are important in a biological sense, their catalytic abilities are also of great interest. The epoxidation of olefins, the oxidation of alcohols to carbonyl compounds and the oxidation of phosphines to phosphine oxides are all catalyzed by Mo-peroxides<12>. The epoxidation and oxidation of olefins is, by far, the most studied reaction. An oxygen from the peroxide group is transferred to the nucleophilic olefin through coordination of the olefin to the metal. The

coordination is usually coplanar with the peroxo group. An intramolecular 1,3 dipolar cycloaddition follows the coordination yielding a five-membered peroxometallocycle which then decomposes to give a molybdenum oxo complex and the epoxide as shown below. If the olefin is terminal this peroxymetallation yields a methyl ketone by a similar mechanism <12>.



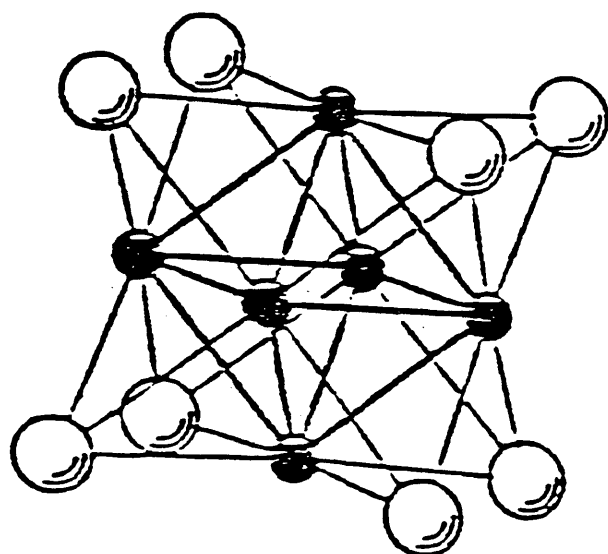


Figure 4. Structure of $[\text{Mo}_6\text{Cl}_8]^{4+}$ cluster.

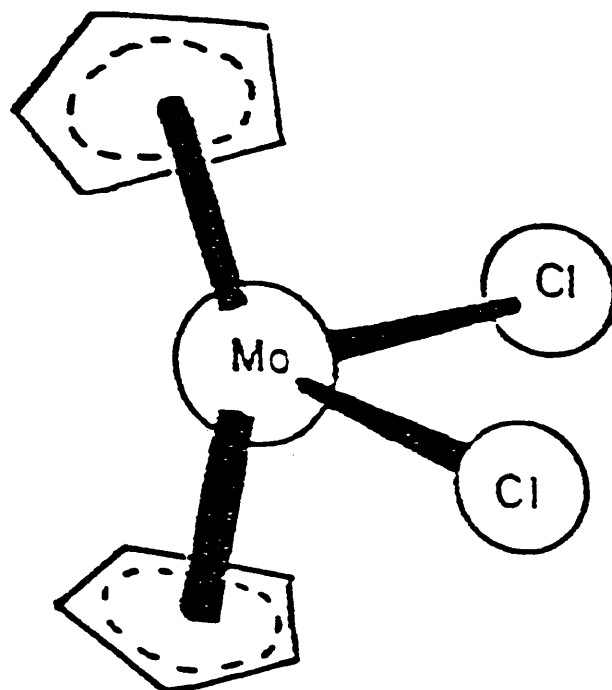


Figure 5. Structure of $(\eta\text{-C}_5\text{H}_5)_2\text{MoCl}_2$

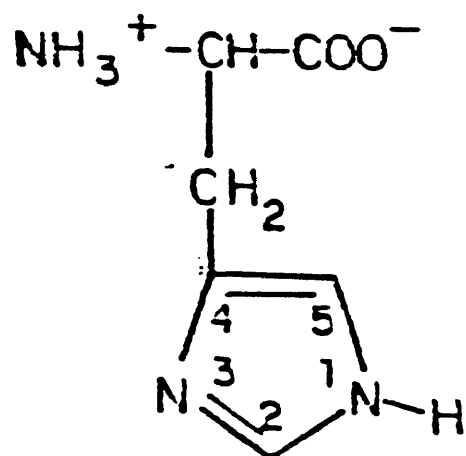


Figure 6. The favored tautomer of histidine.

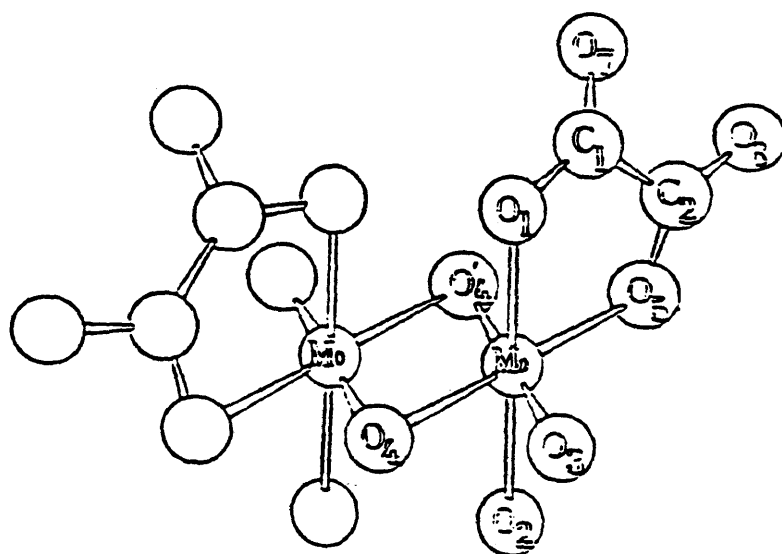


Figure 7. Structure of the $\{[\text{Mn(V)}\text{O}_2(\text{C}_2\text{O}_4)(\text{H}_2\text{O})]_2\text{C}_2\}^{2-}$ anion

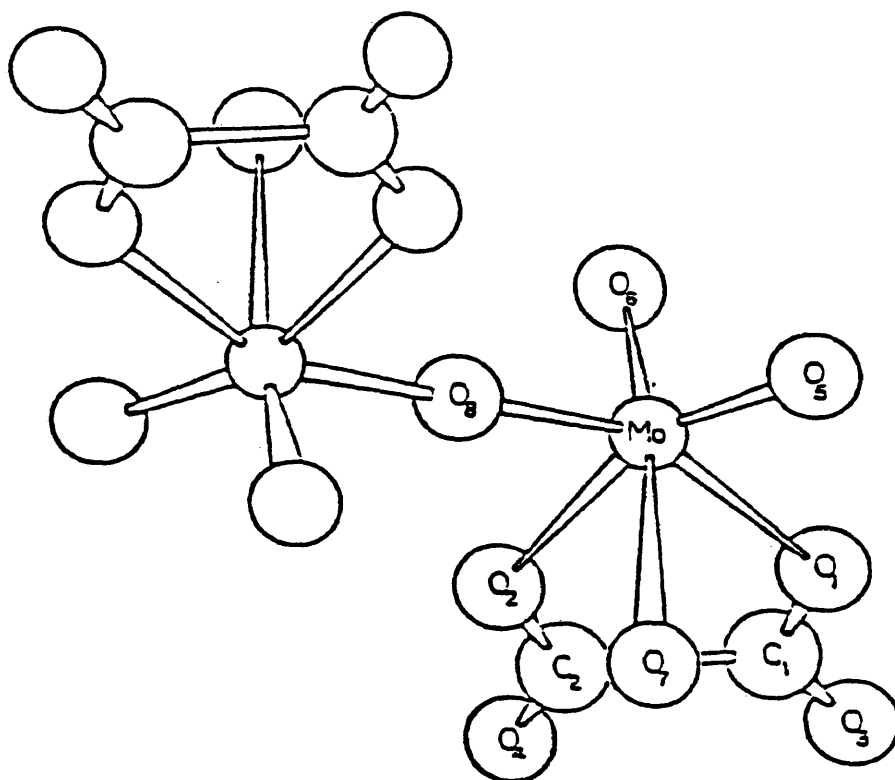


Figure 8. Structure of the $\{[\text{Mo(VI)}\text{C}_2(\text{C}_2\text{O}_4)(\text{H}_2\text{O})]_2\text{C}\}^{2-}$ anion

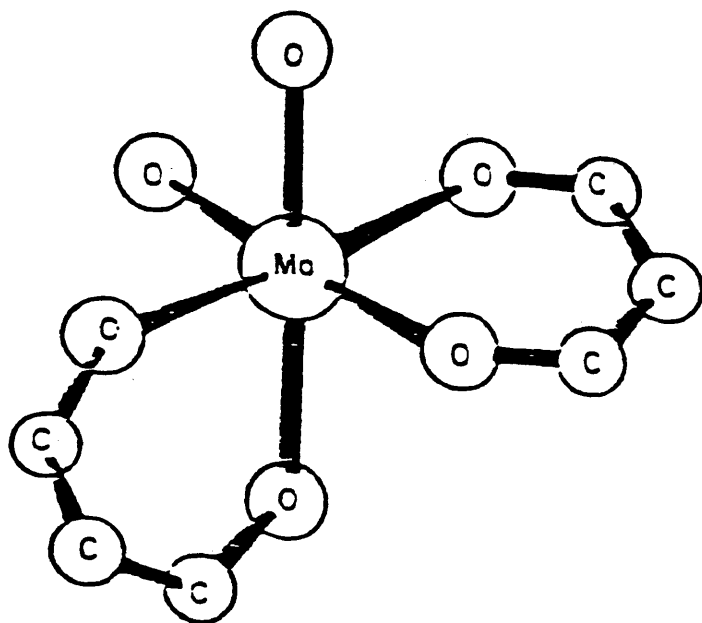


Figure 9. The structure of $\text{Mo(VI)O}_2(\text{acac})_2$

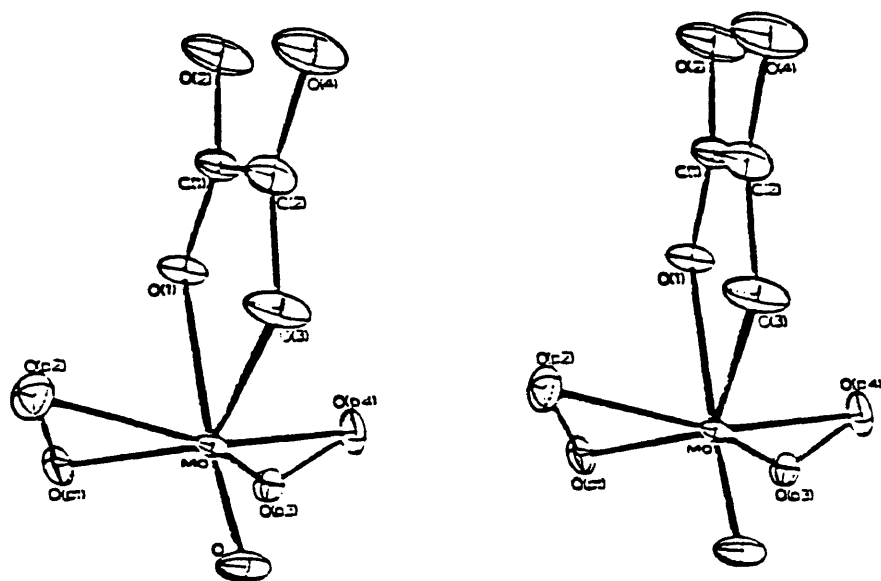
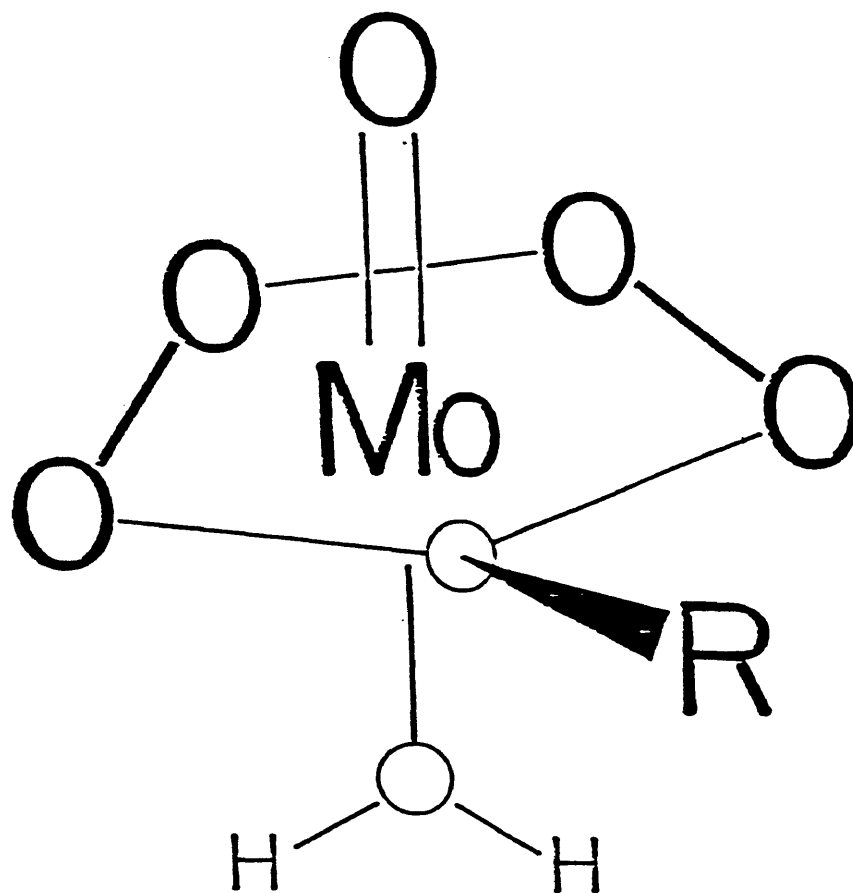
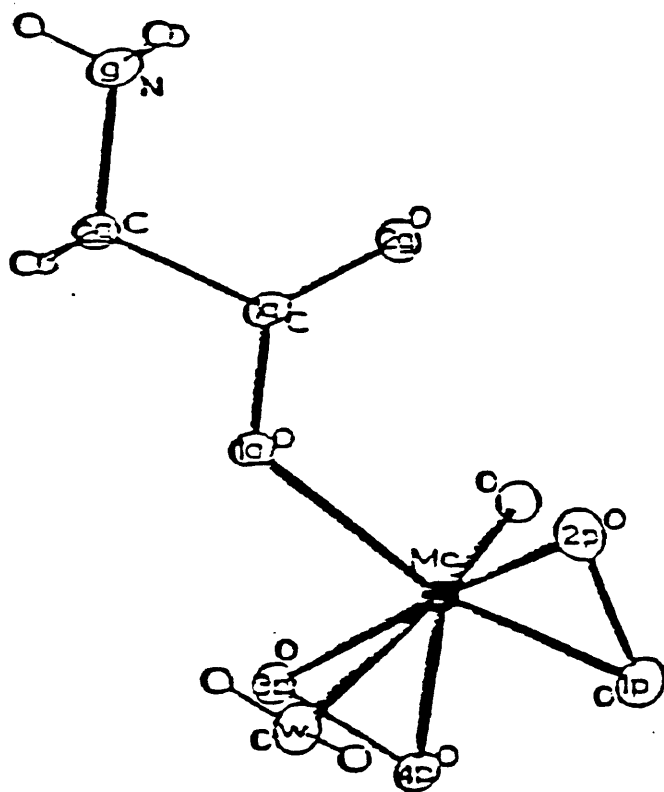


Figure 10. Structure of the $\text{MoC}(\text{O}_2)_2(\text{C}_2\text{O}_4)^{2-}$ anion

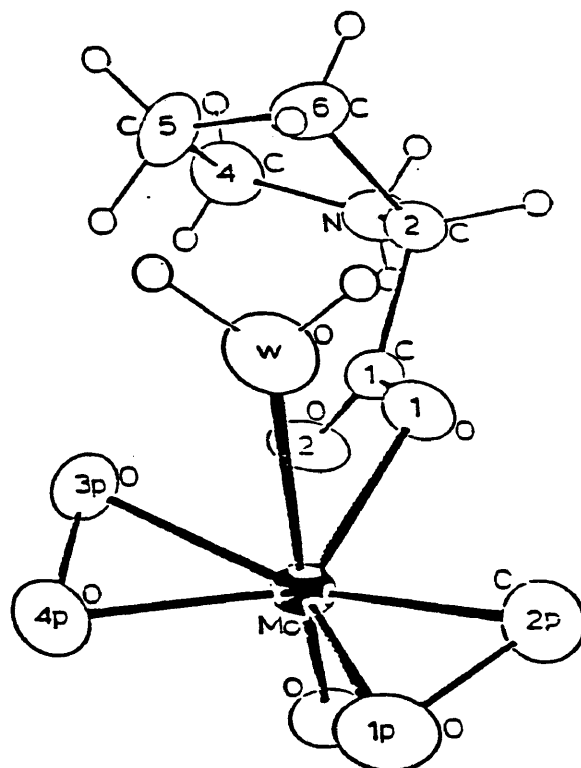
Figure 11

Distorted Pentagonal Bipyramid





(a)



(b)

Figure 12. Structure of $\text{MoO}(\text{O}_2)_2\text{gly}$ (a) and $\text{MoO}(\text{O}_2)_2\text{pro}$ (b).

Table 4

ref. 6

Oxidation States and Stereochemistry of Molybdenum and Tungsten

Oxidation state	Coordination number	Geometry	Examples
Mo ^{-II} , W ^{-II}	5	?	[Mo(CO) ₅] ²⁻
Mo ⁰ , W ⁰ , d ⁶	6	Octahedral	W(CO) ₆ , py ₃ Mo(CO) ₃ , [Mo(CO) ₆] ²⁻ , [Mo(CN) ₆ NO] ³⁻ , Mo(N ₂) ₂ (dipnos) ₂
Mo ^I , W ^I , d ⁵	6 ^a	π -Complex	(C ₆ H ₅) ₂ Mo ⁺ , <i>h</i> ³ -C ₃ H ₅ , MoC ₆ H ₆
	7 ^a	?	(<i>h</i> ³ -C ₃ H ₅) ₂ Mo(CO) ₂
	6	?	MoCl(N ₂) ₂ (dipnos) ₂
Mo ^{II} , W ^{II} , d ⁴		π -Complex	<i>h</i> ³ -C ₃ H ₅ , W(CO) ₅ Cl
	5	See text	[Mo(OCOCH ₃) ₂] ₂ , Mo ₂ Cl ₄ ²⁺
	6	Octahedral	Mo(dians) ₂ X ₂ , Mo(CO) ₂ (dians) ₂
	7	?	[Mo(dians) ₂ (CO) ₂ X] ⁺ , [Mo(CO) ₂ (dians)Br] ₂
	9	Cluster compounds	Mo ₆ Cl ₁₂ , W ₆ Cl ₁₂
Mo ^{III} , W ^{III} , d ³	6	Octahedral	[Mo(NCS) ₆] ³⁻ , [MoCl ₆] ³⁻ , [W ₂ C ₉] ³⁻
	7	?	[W(dians)(CO) ₂ Br] ₂ ⁺
	8	Dodecahedral (?)	[Mo(CN) ₇ (H ₂ O)] ⁴⁻
Mo ^{IV} , W ^{IV} , d ²	8 ^a	π -Complex	(<i>h</i> ³ -C ₃ H ₅) ₂ WH ₃ , (<i>h</i> ³ -C ₃ H ₅) ₂ MoCl ₂
	9 ^a	π -Complex	(<i>h</i> ³ -C ₃ H ₅) ₂ WH ₃
	4	Dist. tetrahedral	Mo(NMe ₂) ₄
	6	Octahedral	[Mo(NCS) ₆] ³⁻ , [Mo(dians) ₂ Br ₂] ²⁺ , WBr ₄ (MeCN) ₂ , MoOC ₂ (PR ₃) ₃
	6	Trigonal prism	MoS ₂
	8	Dodecahedral or square antiprism	[Mo(CN) ₈] ⁴⁻ , [W(CN) ₈] ⁴⁻ , Mo(S ₂ CNMe ₂) ₄ , W(8-quinolinolate) ₄ ^b
Mo ^V , W ^V , d ¹	5	trp	MoCl ₅ (S)
	6	Octahedral	Mo ₂ Cl ₁₀ (S), [MoOC ₂] ³⁻ , WF ₆
	8	Dodecahedral or square antiprism	[Mo(CN) ₈] ³⁻ , [W(CN) ₈] ³⁻
Mo ^{VI} , W ^{VI} , d ⁰	4	Tetrahedral	MoO ₄ ²⁻ , MoO ₂ Cl ₂ , WO ₄ ²⁻ , WO ₂ Cl ₂
	5?	?	WOCl ₄ , MoOF ₄
	6	Octahedral	MoO ₆ , WO ₆ in poly acids, WCl ₆ , MoF ₆ , [MoO ₂ F ₄] ²⁻ , MoO ₃ (distorted), WO ₃ (distorted)
	7	Distorted pentagonal bipyramid	WOCl ₄ (dians), K ₂ [MoO(O ₂)ox]
	8	?	MoF ₈ ²⁻ , WF ₈ ²⁻
	9	?	WH ₆ (Me ₂ PhP) ₃

^a If C₆H₅ and *h*³-C₃H₅ occupy three coordination sites.^b W. D. Bonds, Jr. and R. D. Archer, *Inorg. Chem.*, 1971, 10, 2057.

Table 5
Mo(VI)-peroxo complexes

Formula	Reference
$\text{MoO}(\text{O}_2)(\text{dipic}) \cdot \text{H}_2\text{O}$	12
$\text{MoO}(\text{O}_2)[\text{PhCON}(\text{Ph})\text{O}]_2$	12
$(\text{NH}_4)_3[\text{MoO}(\text{O}_2)\text{F}_4]$	12
$\text{MoO}(\text{O}_2)_2\text{HMPA} \cdot \text{H}_2\text{O}$	12
$\text{K}_2[\text{MoO}(\text{O}_2)_2(\text{C}_2\text{O}_4)]$	42, 43
$\text{MoO}(\text{O}_2)_2\text{gly} \cdot \text{H}_2\text{O}$	TBP*
$\text{K}_2[\text{MoO}(\text{O}_2)_2\text{citrate}] \cdot \text{H}_2\text{O}$	TBP*

dipic= dipicolinic acid

HMPA= hexamethylphosphorictriamide

* - to be published C. Djordjevic et. al.

2.3 Transition metal complexes of imidazole

The imidazole ring (figure 13) is biologically important in many ways. It is the side chain or R-group of the amino acid histidine<26>. It can function as a ligand to many transition metals in numerous biologically important complexes. Imidazole, along with many of its derivatives, function in the iron-heme system of hemoglobin and myoglobin, in vitamin B₁₂, and several other metalloproteins<45>.

The 1,3 diazole ring is actually the systematic name for imidazole. It is an aromatic heterocycle and like most aromatic systems it is planar. It has structural similarities to both pyrrole and pyridine as seen in figures 14 and 15. It therefore has properties of both of these molecules. The N-1, in fact, is referred to as the "pyridine nitrogen" and N-3 is called the "pyrrole nitrogen". The aromatic p-system is composed of six electrons- one from each carbon, one from the pyridine nitrogen and two from the pyrrole nitrogen <46,47>.

Because the two electrons from the pyrrole nitrogen are part of the aromatic sextet, they cannot be involved in bonding with transition metals without disrupting the π -system. Bonding with transition metals will therefore take place primarily at the pyridine nitrogen in neutral

imidazole <45>.

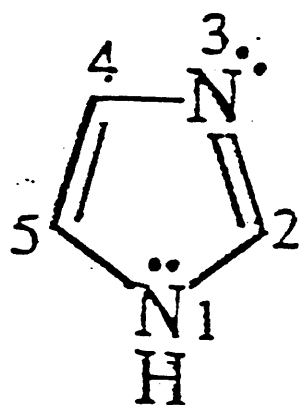


Figure 13. Imidazole

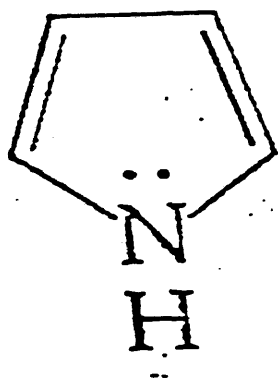


Figure 14. Pyrrole

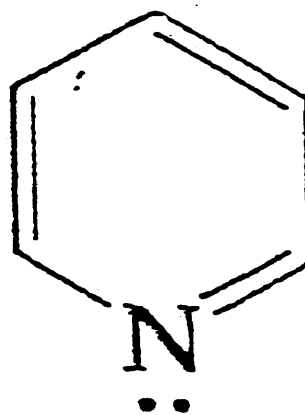
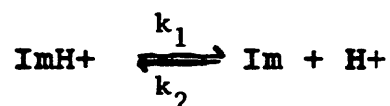


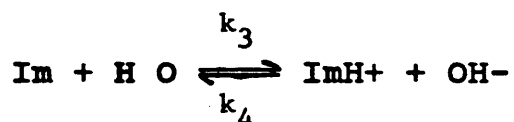
Figure 15. Pyridine

Imidazole is an amphoteric species. It can be protonated at N-3 ($pK_a = 7.1$ @ 25 C, $\mu = 0.2$), acting as a moderately strong base while it can also lose a proton from N-1 to act as a weak acid ($pK_a = 14.2-14.6$). In both cases the ionic species remains aromatic and can still form complexes. In the cationic species the proton can be replaced by a metal as shown in figure 16. The anion has two potential binding sites which are chemically equivalent (figure 17). As an anion the imidazole can serve as a bridging ligand<45>.

In aqueous solutions imidazole tautomerizes without losing its aromaticity via a proton exchange with the solvent. In acidic media the reaction is as follows:



where $k_1 = 10^{3.2} \text{ sec}^{-1} \text{ M}^{-1}$ and $k_2 = 10^{10.2} \text{ sec}^{-1} \text{ M}^{-1}$ indicating that, as written, the reverse reaction is favored thermodynamically. In basic solutions the reaction is:



with $k_3 = 10^{3.4} \text{ sec}^{-1} \text{ M}^{-1}$ and $k_4 = 10^{10.4} \text{ sec}^{-1} \text{ M}^{-1}$. again the reverse reaction is favored<45>. In near neutral solutions at equilibrium an ylide is formed by the

deprotonation of C-2 but it is not a major component of the aqueous mixture. The exchange of the C-2 proton with the solution has a half-life of 109 minutes at 65 C. A summary of the species in imidazole in aqueous solution is given in figure 18 <45>.

As a ligand to transition metals, imidazole exhibits great flexibility. Though it is planar, the metal-N(im) bond can be as great as 30° from the plane of the ligand<48>. This usually occurs because of steric hindrance or hydrogen bonding of the pyrrole nitrogen. In an unhindered complex the metal-N(im) bond will tend to be coplanar with the ligand. Electronic factors do not seem to govern the rotation of the imidazole ring. This flexibility as a ligand may be one of the reasons that imidazole, as itself or as the side-chain of histidine, is a good binding site for metals in proteins<49>.

Another important factor making imidazole a good ligand is the fact that it can form both σ - and π -bonds with metal ions. Sigma bonding is, by far, the most important form of bonding though π -bonding has been shown to have a substantial effect in certain cases<49>.

$[\text{Cu}(\text{ImH})_4]\text{I}_2$ is an especially stable complex due to the presence of imidazole. The coordination of the complex (a distorted octahedron) is such that the plane of the four Cu-N(im) bonds is perpendicular to the plane of each imidazole molecule. This orientation favors a $d_{xy}-p_{\pi}$

orbital overlap. The unpaired electron from the copper is delocalized into the imidazole rings. See figure 19<50>. In the presence of iodine, Cu(II) is usually reduced to Cu(I) via the reaction $\text{Cu(II)} + \text{I}^- \rightarrow \text{Cu(I)} + 1/2 \text{I}_2$. The π -bonding ability of the imidazole stabilizes the complex <49>.

In its anionic form imidazole serves as a bridging ligand for many divalent metal ions forming insoluble polymers of the form $\text{M(II)}[(\text{im})_2]_n$ where $\text{M(II)} = \text{Zn(II)}, \text{Co(II)}, \text{Cu(II)}$ <49>, Fe(II) or Ni(II) <45>. For $\text{Zn}[(\text{im})_2]_n$ each zinc atom is coordinated in a tetrahedral to four different imidazoles. The polymer is composed of puckered rings of four zinc atoms and four imidazoles. Two bonds from each zinc are part of the ring. The third bond links the rings into sheets and the fourth connects the sheets into a three-dimensional network<51>. The copper polymer exists in three different varieties- one of which is very close to a square-planar arrangement<45>. This form of the copper polymer and the zinc polymer are shown in figure 20 <51>.

The imidazolate bridge is also observed in several other complexes either in conjunction with other neutral imidazoles or in mixed-ligand complexes. In an alkaline solution with an im:Cu ratio of 8:1 a perchlorate salt with the formula $\text{Cu}_3(\text{im}^-)_2(\text{imH})_8(\text{ClO}_4)_4$ precipitates. Along with the obviously different species of imidazole there are

two different types of copper present as well. One Cu atom is oriented in a square plane with two bridging imidazoles and two neutral imidazoles while the other two are in a very distorted square plane with three neutral imidazoles and one imidazolate bridge. The Cu-N(im) bond lengths vary from 1.30 to 1.40 Å <45>.

In $[\text{Cu}_2\text{bpim}(\text{imH})]_2(\text{NO}_3)_4 \cdot 4\text{H}_2\text{O}$ (bpim=4,5-bis[(2-(2-pyridyl) ethylimino)methyl]imidazolate) the integrity of the imidazolate bridge is maintained between pH 3.5 and 11.5. At a lower pH the anion is protonated and at higher pH values it competes with hydroxide ions. Four protons can be reversibly titrated in a solution of $[\text{Cu}_2\text{bpim}(\text{imH})]$ which correspond to the protonation of the imidazoles that connect the two monomeric units to give two equivalents of the imidazolium ion (imH_2^+) <52>.

The imidazolate ion has also been shown to serve as a bridge between two different metal ions such as Co(II) and Cu(II) in $[(\text{PMDT})\text{Cu}(\text{im})\text{Co}(\text{NH}_3)_5](\text{ClO}_4)_4$ where PMDT=1,1,4,7,7 pentamethyldiethylenetriamine. In this heterobimetallic complex the bond lengths for the metal-N(im) bonds are 1.933 Å for Co(II) and 1.954 Å for Cu(II) <53>.

Hexacoordinate imidazole complexes have been reported for several metals with various salts. Some examples are: $[\text{Mn}(\text{imH})_6]\text{Cl}_2 \cdot 4\text{H}_2\text{O}$, $[\text{Zn}(\text{imH})_6]\text{Cl}_2 \cdot 4\text{H}_2\text{O}$, $\text{Ni}(\text{imH})_6(\text{NO}_3)_2$ <45>.

Nitrate salts of Cd(II) and Co(II)<45>, a hydrated carbonate salt of Co(II)<54> and a "hydroxide nitrate tetrahydrate" of Cd(II) of disputed formula have been reported. The complex originally reported as $\text{Cd}(\text{im})_6(\text{OH})(\text{NO}_3) \cdot \text{H}_2\text{O}$ <55> has been shown to actually be $[\text{Cd}(\text{im})_6](\text{CO}_3) \cdot 5\text{H}_2\text{O}$ <80>. In most cases coordination about the metal is a distorted octahedron. The three very similar nitrate salts are a good example. The ion $\text{M}(\text{II})(\text{im})_6^{+2}$ has threefold symmetry with one of the axes slightly compressed in the octahedral. The trans imidazoles are coplanar and are rotated 24° from the plane defined by the metal and the four imidazole nitrogens. The rotation about the plane serves to minimize the steric hindrance of the rings<45>.

Not all transition metal complexes with imidazole are six-coordinate. At pH 5, with a Cu(II):im ratio of 1:2, a crystalline complex with the formula $\text{Cu}(\text{im})_2\text{Cl}_2$ is precipitated. In this complex the copper atom is five-coordinate with a square-pyramid structure. The plane is made up of two N(im) atoms and two Cl atoms. The apex of the pyramid is a Cl that bridges two copper atoms. The bridging Cl of one unit lies in the square plane of the other unit that it bridges. Figure 21 shows the structure of this complex. The copper atom lies 0.18\AA out of the plane formed by the Cl and N(im) atoms.<57>.

When excess imidazole is present at pH 7.5-8.0, a

different crystal precipitates with the formula: $\text{Cu}(\text{imH})_2(\text{im-})\text{Cl}$. The copper is again bridged but this time by imidazolate ions. The remaining coordination sphere is filled by two neutral imidazoles and one chlorine. The $\text{Cu-N}(\text{im-})$ bond lengths (1.986 and 1.963 Å) are significantly shorter than the $\text{Cu-N}(\text{imH})$ bonds which are 2.058 Å. The polymer chains are held together by hydrogen bonds<58>. A summary of some transition metal complexes with imidazole is given in Table 6<45>.

Several mixed-ligand complexes containing imidazole and aspartic acid have been reported. The structures of both $[\text{Cu}(\text{II})(\text{L-asp})(\text{imH})] \cdot 2\text{H}_2\text{O}$ and $\text{Ni}(\text{II})(\text{L-asp})(\text{im})_3$ have been characterized<59,60> while solution studies on the formation of $\text{Cu}(\text{II})(\text{im})(\text{asp})$ and $\text{Cu}(\text{II})(\text{im})_2(\text{asp})$ have been examined<48>. In $\text{Cu}(\text{L-asp})(\text{imH}) \cdot 2\text{H}_2\text{O}$ the copper is coordinated in a distorted square pyramid with three aspartate ions and one imidazole in a polymeric, two-dimensional network. Each asp ion is bidentate and forms a bridge to another copper<59>. For the $\text{Ni}(\text{II})(\text{L-asp})(\text{imH})$ complex, the $\text{Ni}(\text{II})$ is coordinated in a distorted octahedron with the aspartate ion acting as a tridentate ligand and the remaining three coordination sites occupied by the three neutral imidazoles<60>.



Figure 16. Cationic forms of imidazole

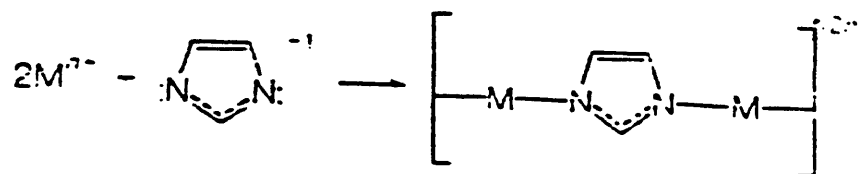


Figure 17. Anionic form of imidazole and as a metal bridge.

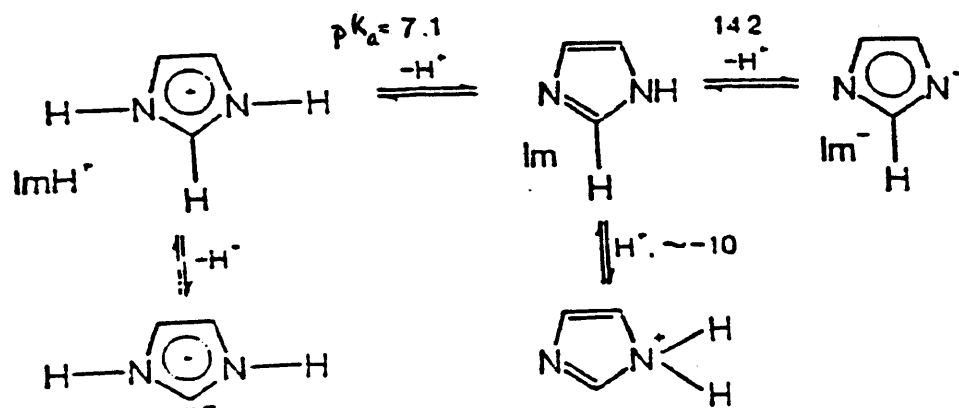


Figure 18. Species of imidazole in aqueous solution.

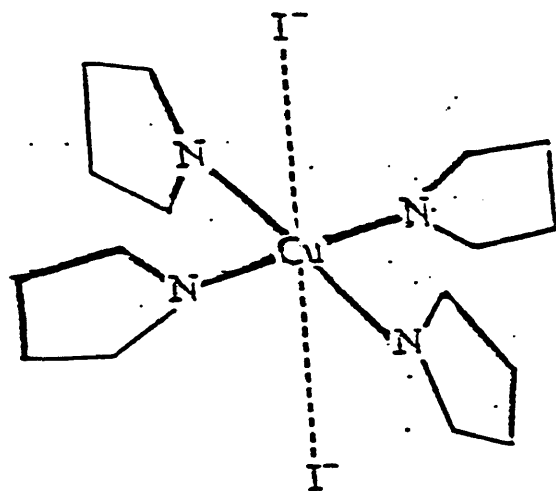
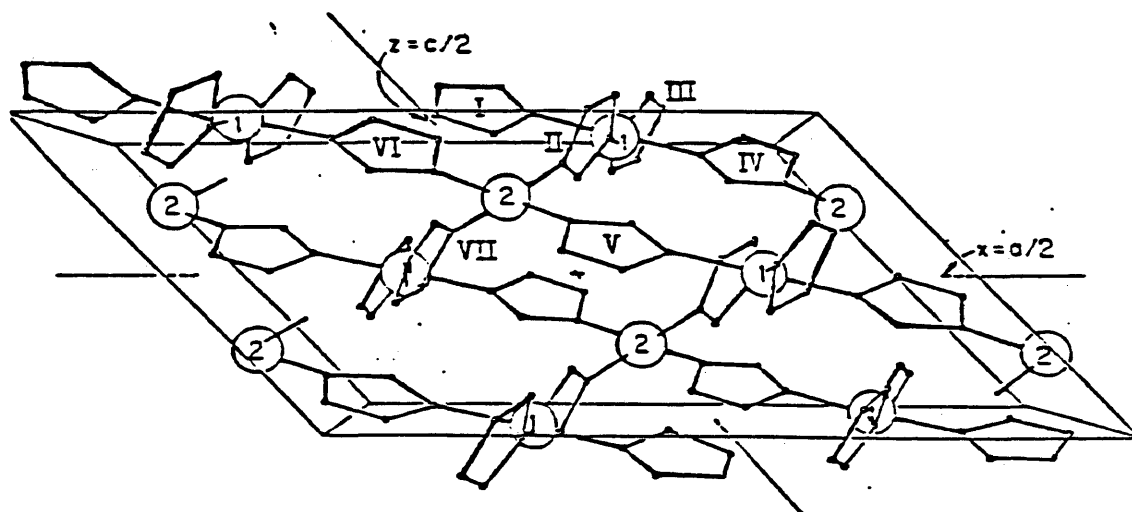
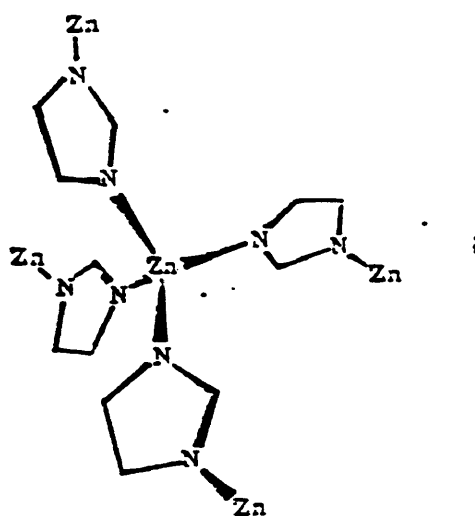


Figure 19. Structure of $\text{Cu}(\text{imH})_4 \text{I}_2$



(a)



(b)

Figure 20. Structures of the polymers Cu(II)(im)_2 (a) and Zn(im)_2 (b).

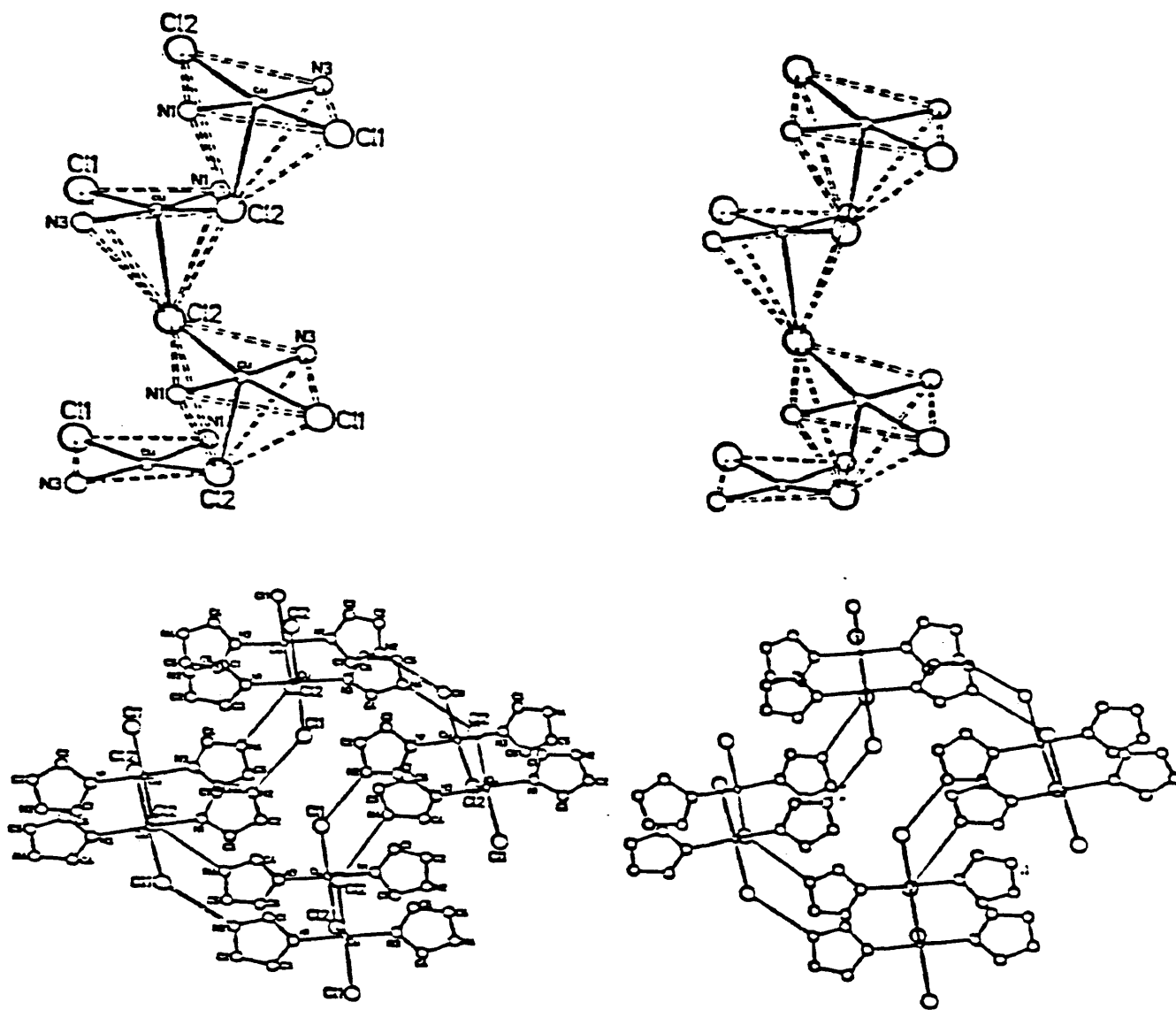


Figure 21. Structure of the five-coordinate $\text{Cu}(\text{im})_2\text{Cl}_2$ polymer.

Table 6
Metal Complexes with imidazole

ref 45

Formula (M(II) (im) _x -2	Anion	Structure
Mn(im)	Br, Cl	poly. oct.
Mn(im) ₂	Cl, Br, I, NCS	poly. oct.
Mn(im) ₄	Cl, Br, I, ClO ₄ , NCS	dist. oct.
Co(im)	Cl	poly. oct.
Co(im)	Br, I	dist. tet.
Co(im) ₂	Cl, Br, I	tet.
Co(im) ₂	NO	oct.
Co(im) ₂	NCS	several
Co(im) ₂	NCSe	poly. oct.
Co(im) ₄	ClO ₄	tet.
Co(im)	NCO, NCS, NCSe	oct.
Ni(im)	Cl, Br	poly. oct.
Ni(im)	I	dist. tet.
Ni(im) ₂	Cl, Br	poly. oct.
Ni(im)	I	dist. tet.
Ni(im) ₄	Cl, Br, I	oct. or sq.
Zn(im) ₂	Cl, Br, I	tet.
Zn(im) ₂	NO ₃	?
Zn(im) ₄	NO ₃	dist. oct.

poly= polymeric, dist.= distorted, oct.= octahedral
tet.= tetrahedral

2.4 Transition metal complexes with histidine

Much of the complexing behavior of histidine (Figure 6) with transition metals has already been covered in the section on imidazole because much of the coordination of histidine occurs through imidazole <45,61>.

Unlike imidazole, histidine has three potential coordination sites that become available as the pH increases. The carboxyl group has the lowest pKa at 1.9. Imidazolium has a pKa of 6.1. The amino group is deprotonated next with a pKa of 9.1 and finally the pyrrole nitrogen is deprotonated (pKa=14.4) <45,61>. The pyrrole nitrogen does not usually participate in bonding to transition metals. Figure 22 summarizes the species of histidine in aqueous solution over a wide pH range <45>.

One would assume that the order of deprotonation of histidine would also be the order in which the donor atoms would be used in metal binding. In this manner it would be expected that the steps of metal-histidine complexation would be the following: First there would be unidentate coordination by the carboxyl oxygen. The pyridine nitrogen from the imidazole ring would then coordinate to form a seven-membered ring. Next would be the coordination of the amino group to make histidine a tridentate ligand. Finally, the pyrrole nitrogen would be deprotonated but it

is unlikely that it would also coordinate<49>.

Formation of a seven-membered ring is generally unfavorable energetically. In order to overcome this the hydrogen on the pyrrole nitrogen can tautomerize to N-3 and N-1 can become the pyridine nitrogen. Coordination of the O(carboxyl) to the new pyridine nitrogen results in a much more favored six-membered ring. Carbon-13 and nitrogen-15 n.m.r. spectroscopy have determined that the N-1 H tautomer predominates by a 4 to 1 ratio over the N-3 H tautomer. Figure 6 depicts the favored tautomer. In this form a six-membered ring can be formed with the amino nitrogen and the N-3 pyridine nitrogen<61>.

Most of the crystal structures that have been published are for complexes that have been formed in the pH range where histidine is a tridentate ligand. This does not shed much light on the order of chelation of the ligand. Some representative complexes are shown in figure 23. Co(II)(L-his)_2 and Ni(II)(L-his)_2 are octahedrally coordinated. In the zinc complexes the structure is based more on the tetrahedron with strong Zn-N(im) and Zn-N(amino) bonds and rather weak Zn-O(carboxyl) interactions<49>.

A solution study of Co(II) complexes with histidine over a wide pH range gives some interesting insights into the coordinating ability of the ligand. A proton magnetic resonance study of the aqueous Co(II)-his complexes was

done over the pH range of 1 to >11. The data indicated that there were four distinct species present over the range (see figure 24). Below pH 4 the histidine is coordinated in a unidentate manner via the O(carboxyl). Between pH 4 and 11 two octahedral complexes are formed with Co:his ratios of 1:1 and 1:2. In both cases the histidine acts as a tridentate ligand. For pH>11 a tetrahedral complex is formed where the both histidines are coordinated through the amino group and the N(im) <62>.

One p.m.r. study has been done for a complex where the histidine is actually bidentate. A 1:2 Pt-his complex has been shown to have square planar geometry with coordination through the N(amino) and N(im). The complex remains unchanged over the pH range of 1 to 12. At high pHs the carboxyl and imidazolium groups are deprotonated but the coordination remains the same. Figure 25 shows the structure of the complex at both high and low pH values <49>.

Pd(II) also forms a complex that is analogous to $\text{Pt}(\text{his})_2$ in that the ligand is bidentate and the complex is square planar. These structures show that the order of deprotonation is not always the order in which metal binding will take place. In the Pt(II) and Pd(II) complexes one reason for this is the increase in crystal field stabilization energy (CFSE) that occurs when the N(im) and N(amino) are coordinated in a square planar

configuration to the metal ion. The other, probably more important, reason is that a six-membered ring is much easier to form and is much more stable than the seven membered ring that could form instead<49>.

Though no Mo(VI)-his complexes have yet been isolated in crystalline form<36>, the structure of a Mo(V) complex, $\text{Mo(V)}_2\text{O}_4(\text{L-his})_2 \cdot 3\text{H}_2\text{O}$ has been determined by X-ray methods. The complex (figure 26) is dimeric with the two Mo atoms connected by two bridging oxygens. The histidine is, as usual, a tridentate ligand that is coordinated via the O(carboxyl), the N(im) and the N(amino). Each Mo(V) has a distorted octahedral geometry <63>.

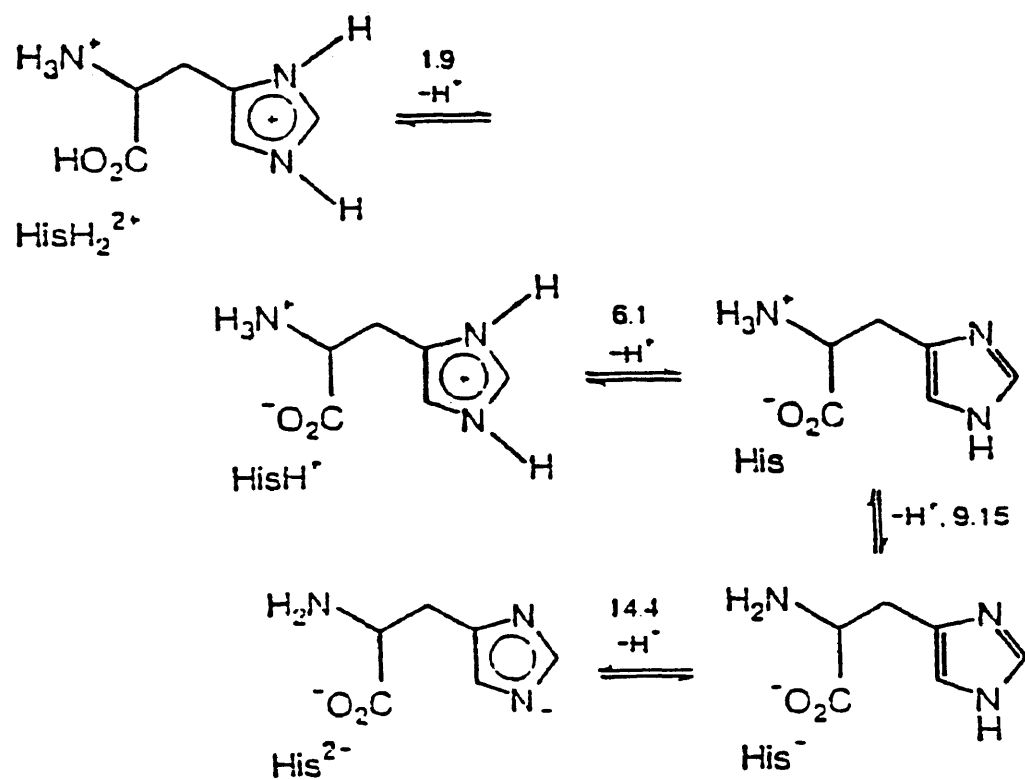
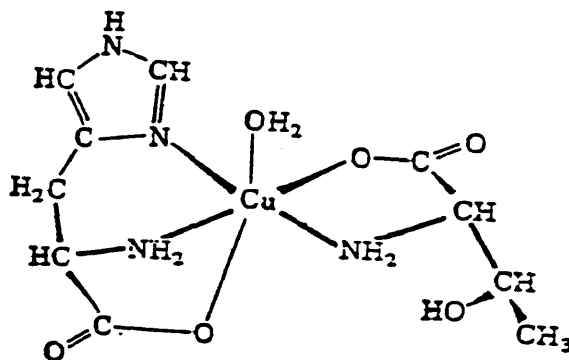
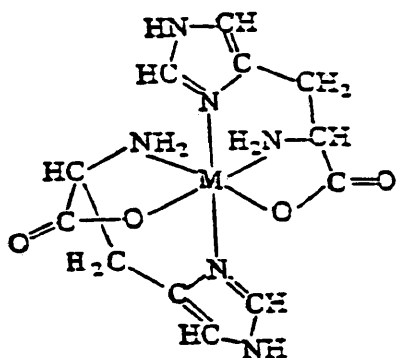
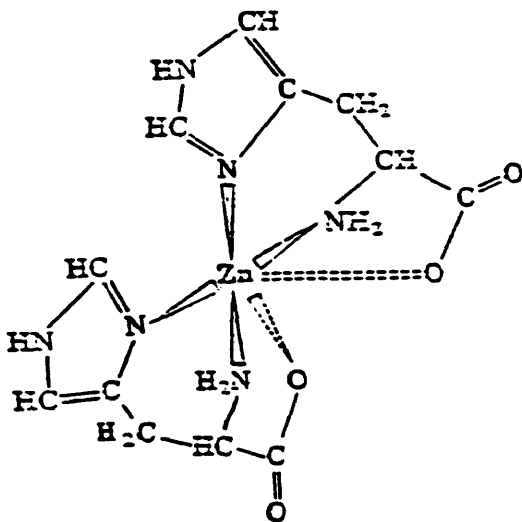


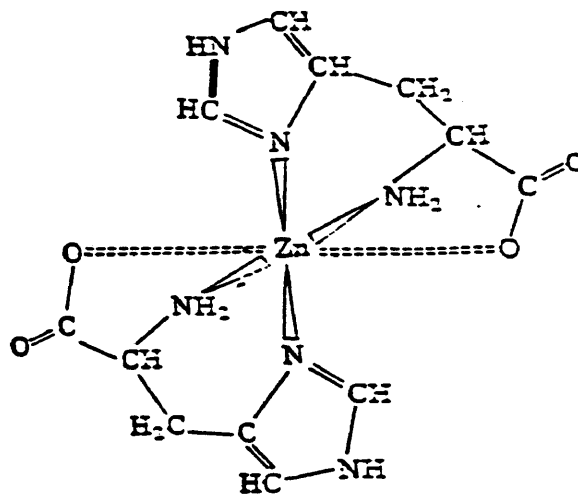
Figure 22. Species of histidine in aqueous solution.
Equilibrium constants are expressed as pK_a
values above the arrows.



$M(L-His)_2$, $M = Co(II), Ni(II)$



(a)



(b)

$Zn(L-His)_2$ in (a) $Zn(L-His)_2 \cdot 2H_2O$ and (b) $Zn(D-His)(L-His) \cdot 5H_2O$

Figure 23. Some representative transition metal-histidine complexes.

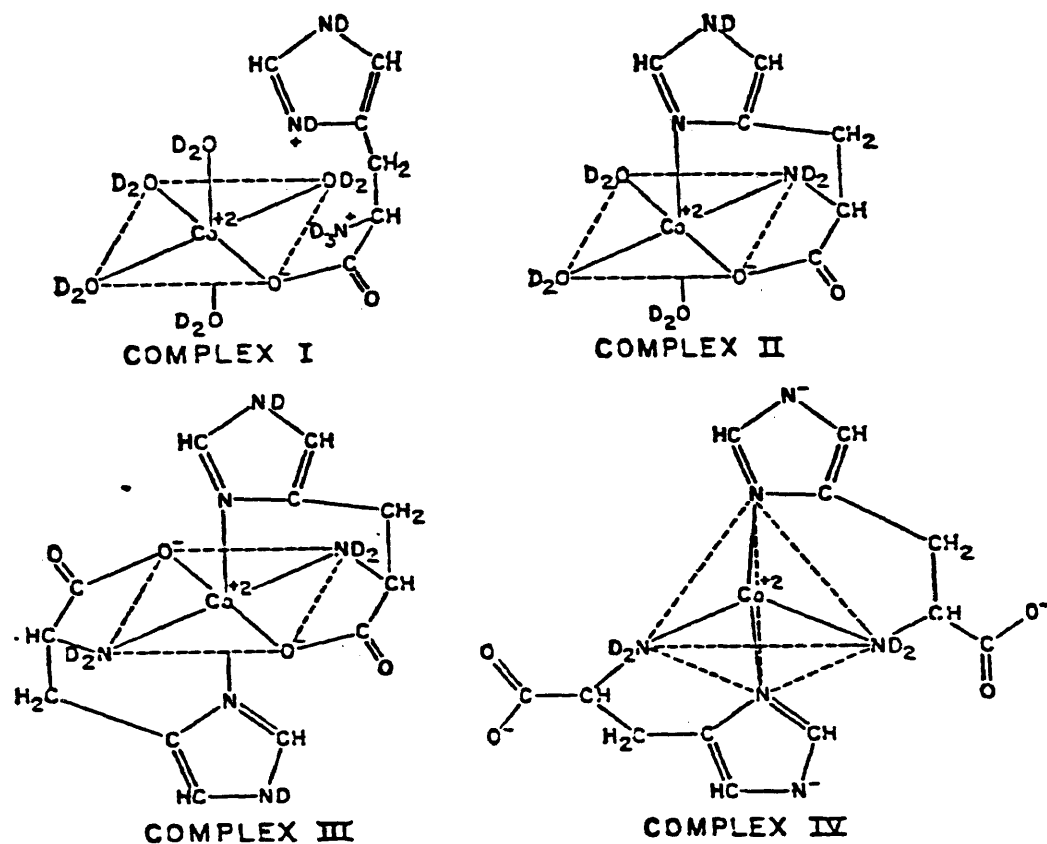
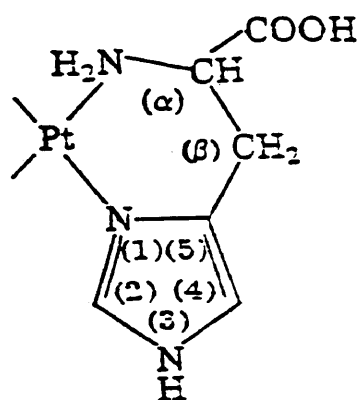
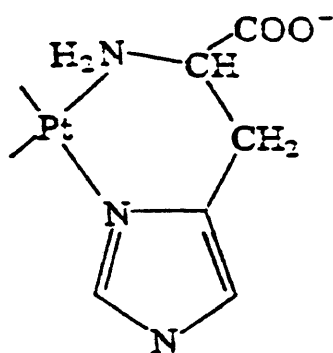


Figure 24. Structures of Co(II) -histidine complexes.



Coordination in $[\text{Pt}(\text{HHis})_2]^{2+}$



Coordination in $[\text{Pt}(\text{H}_{-1}\text{His})_2]^{2-}$

Figure 25.

3 Results and Discussion

3.1 Peroxo imidazole vanadates

Peroxo complexes of vanadium with various organic ligands can act in many ways, as has already been discussed. Several such complexes have already been synthesized but, to date, no oxoperoxoimidazole vanadates(V) have been reported.

We have attempted to isolate crystalline oxoperoxoimidazole vanadates(V) from aqueous solutions of NH_4VO_3 or $\text{V}_2\text{O}_5 \cdot \text{H}_2\text{O}$, imidazole and usually K^+ or NH_4^+ salts. While no complexes have been separated, the possibility of eventually obtaining a crystalline compound should not be excluded. Due to time limitations, this system was not studied as thoroughly as possible. Our initial investigations have shown that, under similar conditions, imidazole complexes do not form as readily with V(V) as they do with Mo(VI). This observation has been made with numerous other ligands as well.

In most cases, the products that were obtained from the various vanadium-peroxo-imidazole systems were only forms of vanadates with no ligands that only rarely seemed to contain peroxide. In many attempts the V(V) was reduced to V(IV) or V(III) due to overheating or simply standing in

solution too long before precipitation. The reduction could easily be determined by a color change from yellow or orange to black or brown.

Infrared spectra were taken for all products that had not been reduced. Since it was apparent that no ligand was present on the vanadium, no further analysis was done on the products. In only one case was there any evidence that there was some ligand present but subsequent Ce(IV) titration for peroxide showed that there was no peroxide present. This product could not be reproduced again in the time given to this system.

3.2 Peroxo imidazole molybdates

The coordination of imidazole and imidazole derivatives to transition metals and transition metal complexes in chemical and biological systems has been studied extensively.<45> Heteroligand and mixed ligand complexes have been reported with Cu(II) <45,48,52,53,59,64-66>, Fe(II) <67-70>, Co(II) <53,60,71-73>, Ni(II) <60,73>, Mn(II) <74,75>, Zn(II) <51,74,76>, Rh(II) <77>, U(VI) <78>, and Pt(II) <79>. Imidazole complexes of Mo(VI) have not been reported until now.

We have investigated the complex formation of imidazole with Mo(VI) and have obtained well-crystallized, stable oxo peroxo imidazole complexes with Mo(VI) as well as two impure mixtures. These mixtures came from the systems $K/Mo/O/O_2/im$ and $K/Mo/O/im$.

Two different yellow oxo peroxo imidazole molybdates have been obtained. The first complex is a monooxodiperoxo species with the formula, $MoO(O_2)_2 \cdot im \cdot H_2O$ while the other is a dioxomonoperoxo complex, $MoO_2(O_2) \cdot im \cdot H_2O$. Both were prepared in aqueous solutions of molybdenum trioxide, hydrogen peroxide and the ligand, using surprisingly similar procedures. In both cases a solution of MoO_3 in hydrogen peroxide is prepared. The ligand is dissolved in a small amount of water and is then added to the molybdenum-peroxide solution. The rate at which the

imidazole solution is added, along with the amount of stirring after the addition, usually determines which product will be obtained.

The reason why the rate of addition of the ligand is so crucial is most likely due to the fact that when the ligand is added slowly the metal and peroxide are in excess with respect to the imidazole for the majority of the addition. This allows the diperoxo complex to form instead of the monoperoxo. When the imidazole is added all at once the ligand is present in a larger local concentration which results in the formation of the monoperoxo complex.

The two peroxo compounds were analyzed for C, H, N, O_2^{2-} and Mo content. The x-ray structure of the crystals are in the process of being determined. UV/visible spectra were also run on the complexes. The precipitate obtained from the potassium peroxo system were analyzed for C, H and N content along with peroxide percentage. The precipitate obtained from the potassium oxo system was analyzed for C, H and N. Infrared spectra were obtained for all of the precipitates. The results of $MoO(O_2)_2 \cdot im.H_2O$, will be discussed first.

The yellow prism-like crystals of $MoO(O_2)_2 \cdot im.H_2O$ are formed in acidic aqueous solutions at a pH of 4-6. The crystals dissolve readily in aqueous acids and slowly in water giving a clear yellow solution. In aqueous, basic media the crystals seem to decompose slowly with an

evolution of oxygen leaving a clear, colorless solution. The complex appears to be insoluble in most common organic solvents including CH_2Cl_2 , ethanol, and acetonitrile. The crystals can be ground easily to form mulls. It is most likely a monomer. Figure 27 shows a possible structure for the complex.

On examining the infrared spectrum of the compound and comparing it with that of imidazole it was first observed that the compound has three strong additional broad peaks at 3420, 3230, and 3140 cm^{-1} . Imidazole has only one strong peak in this region at 3120 cm^{-1} that is due to N-H stretching. In most hydrated inorganic crystals lattice water, or water of hydration, absorbs between 3550 and 3200 cm^{-1} <79>. The peaks at 3420 and 3230 cm^{-1} are most likely due to lattice water while the peak at 3140 cm^{-1} is probably due to a combination of both the imidazole N-H stretch and lattice water.

Before research was begun with molybdenum, one Ni(II)-imidazole complex and two known Zn(II)-imidazole complexes <51,76> were prepared and their ir were examined. In this way the spectra of imidazole that is coordinated to various transition metals could be compared. In all spectra, including that of imidazole and $\text{MoO}(\text{O})_2 \cdot \text{im} \cdot \text{H}_2\text{O}$, a strong, sharp peak is observed between 1090 and 1050 cm^{-1} . This is due to C-H deformation in the imidazole ring. <80> (The band assignments for solid imidazole are taken from

Bonsor et. al-⁸⁰.) The ring deformation band at 1540 cm^{-1} in imidazole is shifted to 1580 cm^{-1} in the complex while the peak at 1670 cm^{-1} is shifted to 1650 cm^{-1} in $\text{MoO}(\text{O}_2)\text{im.H}_2\text{O}$. The ring deformations at 1500 and 1480 cm^{-1} are shifted to 1440 and 1430 cm^{-1} . Since there are a great deal of strong peaks in the region between 1100 and 700 cm^{-1} for both imidazole and the complex, it is very difficult to determine where the $\text{Mo}=\text{O}$ and $\text{O}-\text{O}$ stretchings appear. The $\text{Mo}=\text{O}$ stretchings usually appear between 1100 and 900 cm^{-1} while $\text{O}-\text{O}$ absorbs between 900 and 800 cm^{-1} . In $\text{MoO}(\text{O})\text{im.H}_2\text{O}$ the $\text{Mo}=\text{O}$ peak is most likely the strong, sharp band at 960 cm^{-1} . The $\text{O}-\text{O}$ stretch is most likely represented by the strong, broad band at 860 cm^{-1} . Figures 28 and 29 show the spectra of imidazole and $\text{Mo}(\text{O}_2)_2\text{im.H}_2\text{O}$.

UV/visible spectra for the compound were obtained for solutions at pH 1 in an HCl/KCl buffer ($\mu=0.1$), ($\lambda_{\text{max}}=325\text{ nm}$), for solutions in 0.1M KCl ($\text{pH}=4$, 10^{-3}M , $\lambda_{\text{max}}=315\text{ nm}$), and in the solid state in a nujol mull. (Figure 30). Imidazole itself does not show any absorption in the range of 900 to 200 nm in either the solid state or 0.1M KCl solutions at a concentration of 10^{-3}M .

$\text{Ce}(\text{IV})$ titration for peroxide indicates that the complex contains between 19 and 21 percent peroxide. This agrees well with the proposed formula, $\text{MoO}(\text{O}_2)_2\text{im.H}_2\text{O}$. The results of C, H, and N analysis are given in Table 7.

The first crop of prism-like crystals was obtained in

a rather good yield of between 40 and 60 percent. A second, small crop of crystals precipitated later but the crystals were irregular and the ir spectrum indicated that no ligand was present. Seeding the mother liquor with a small crystal of $\text{MoO}(\text{O}_2)_2 \cdot \text{im.H}_2\text{O}$ before the second crop precipitates does not alter the character of the second crop. The decomposition point of the compound was determined to be near 125°C . At this temperature the crystals explode, leaving a whitish residue.

The needlelike crystals of $\text{MoO}_2(\text{O}_2) \cdot \text{im.H}_2\text{O}$ dissolve very slowly in both aqueous acids and water to give clear yellow solutions. In bases the crystals decompose rapidly leaving a colorless clear solution. No significant evolution of gas is observed as with $\text{MoO}(\text{O}_2)_2 \cdot \text{im.H}_2\text{O}$. Grinding the crystals to form nujol mulls is very difficult. This indicates that the compound could be polymeric. A possible dimeric structure of the complex are shown in Figure 31.

The ir spectrum of the complex is shown in Figure 32. It is rather poorly resolved due to the difficulty associated with mulling. Many characteristic absorptions are still apparent though. The broad shoulder between 3650 and 3400 cm^{-1} is most likely due to water in the lattice of the crystal. The shoulder at about 1630 cm^{-1} seems to reinforce the likelihood of water of crystallization. Two C-H deformations remain unshifted at 1099 and 1053 cm^{-1} .

The Mo=O stretch appears at 952 cm^{-1} and the O-O stretch is present at 850 cm^{-1} . One ring deformation band appears to be shifted slightly from 895 cm^{-1} to 890 cm^{-1} . Unlike the diperoxo species, few imidazole bands remain resolved in the monoperoxo complex. The region between 900 cm^{-1} and 400 cm^{-1} is marked by an overall increase in absorbance. This is often due to bridging oxygens between the Mo(VI) atoms and lends more credence to the possibility that the complex is polymeric. Definite proof of the structure lies in the x-ray structure analysis. The small size of the crystals available now makes analysis impossible.

The yield of these crystals is rather low- usually between 12% and 15% for the first crop. A second crop usually precipitates quickly but it seems to be a mixture of the needlelike crystals as well as some irregular yellow crystals. The ir spectra of the second crops are essentially identical to those of the first crops though they are not as well resolved. Ce(IV) titrations gives a rather constant peroxide content of between 13% and 15%. The various second crops were found to contain between 7% and 11% peroxide- implying the presence of a mixture.

UV/visible spectra were run for the complex in the same manner as for the diperoxo complex. At pH 1 the λ_{max} was observed at 320 nm. In the solid state a broad absorption was observed which was centered at $\sim 330\text{ nm}$.

The C, H, N analysis of the compound is given in Table

7 and agrees rather well with the proposed theoretical values.

The system $K/Mo/O/O_2/im$ produced irregular crystals with a peroxide content of about 20%. Inspection of the ir spectrum (Fig. 33) shows a strong peak at 960 cm^{-1} which is most likely due to the $Mo=O$ stretch. The strong peak at 850 cm^{-1} has numerous shoulders. One of the bands within this peak is most probably due to the peroxide stretch. The series of N-H stretches in imidazole that are located between 3200 and 2600 cm^{-1} are either shifted or obscured. A broad water peak is observed at 3350 cm^{-1} . The ring stretches and C-H deformations that remain resolved are greatly decreased in intensity with respect to the $Mo=O$ and O-O bands.

Theoretical calculations of the C, H and N content of the possible complex, $K[MoO(O)_2]_2 \cdot im \cdot H_2O$, gave the following values: C-12%, H-2% and N-9%. Microanalysis of the compound gave values of 7.8%, 1.1%, and 5.9% for C, H and N respectively. The yellow crystals that were obtained are most likely a mixture of some potassium oxoperoxo imidazole molybdate along with some peroxo molybdate salts. The reproducibility of this reaction leaves much to be desired. In the majority of the runs in this system the peroxo molybdates with no ligand was obtained with only traces of the complex present. Due to the impurity of the product no UV/visible spectra were run.

The preparation of a potassium oxo imidazole complex with molybdenum also proved to be rather disappointing. In the infrared spectrum (Fig. 34) there is a broad absorbance between 3600 cm^{-1} and 3100 cm^{-1} that is slightly resolved into a triplet. It is most likely due to a combination of N-H stretches and water of crystallization. Two overlapping peaks are observed at 1635 and 1660 cm^{-1} . It is also probably due to lattice water and N-H stretches. At 1060 cm^{-1} there is a weak peak associated with C-H deformation. This is the same peak that is seen in all of the other molybdenum-imidazole complexes reported here. Overtones from the coordination of the ligand to the metal are seen between 1400 and 1100 cm^{-1} . The strong, broad peak at 900 cm^{-1} with shoulders at 920 cm^{-1} and 870 cm^{-1} could be due to either Mo=O stretching or C-H deformation or both factors. The remaining sharp peak at 840 cm^{-1} is due to C-H deformation.

The predicted values for C, H, and N are 16%, 3%, and 12% respectively but microanalysis found only 2.5% C 0.9% H and 1.8% N. While the theoretical calculations may be slightly off, the C, H and N content is very low nonetheless. A melting point determination is often useful in determining if a product is pure or a mixture. These crystals exhibited no melting point up to 230°C . They did not appear to change physically on heating though the spectrum of the crystals indicated that changes must have

occured. Most noticable was the change in the water and N-H peaks between 3600 and 3100 cm^{-1} . In the unheated product it is very strong with three peaks while after heating it became a very weak broad band without any additional peaks. This indicates that a water of crystallization was driven off.

The system $\text{NH}_4/\text{Mo}/\text{O}/\text{O}_2/\text{im}$ produced small yellow irregular crystals. Its infrared spectrum seemed to indicate that a complex was formed. Ce(IV) titration gave a peroxide content of about 23%. The results of microanalysis though, gave very low C and H contents. The relatively higher N content (Table 7) indicates that this precipitate is probably a mixture of an ammonium peroxo molybdate salt with a small amount of some imidazole complex.

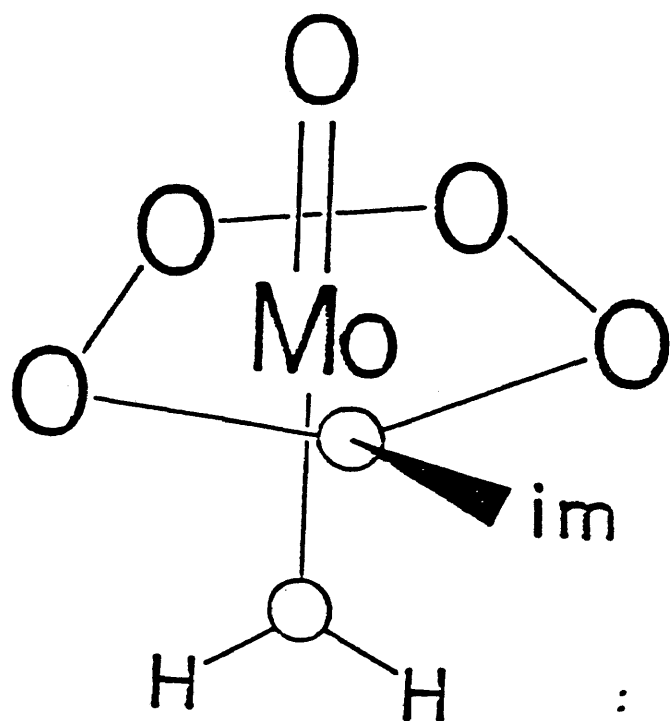


Figure 27. Possible structure of $\text{MoO}(\text{O}_2)_2\text{im}\cdot\text{H}_2\text{O}$

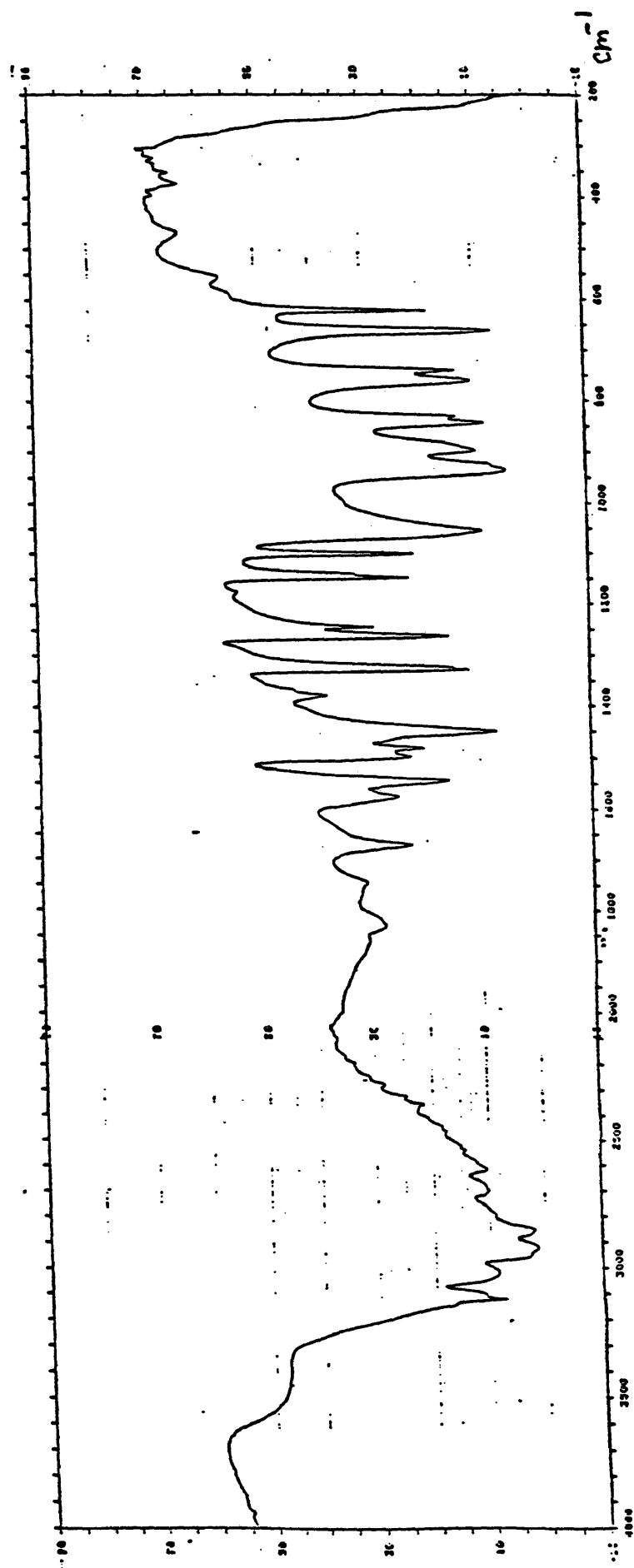


Figure 28. Infrared spectrum of imidazole (Nujol mull).

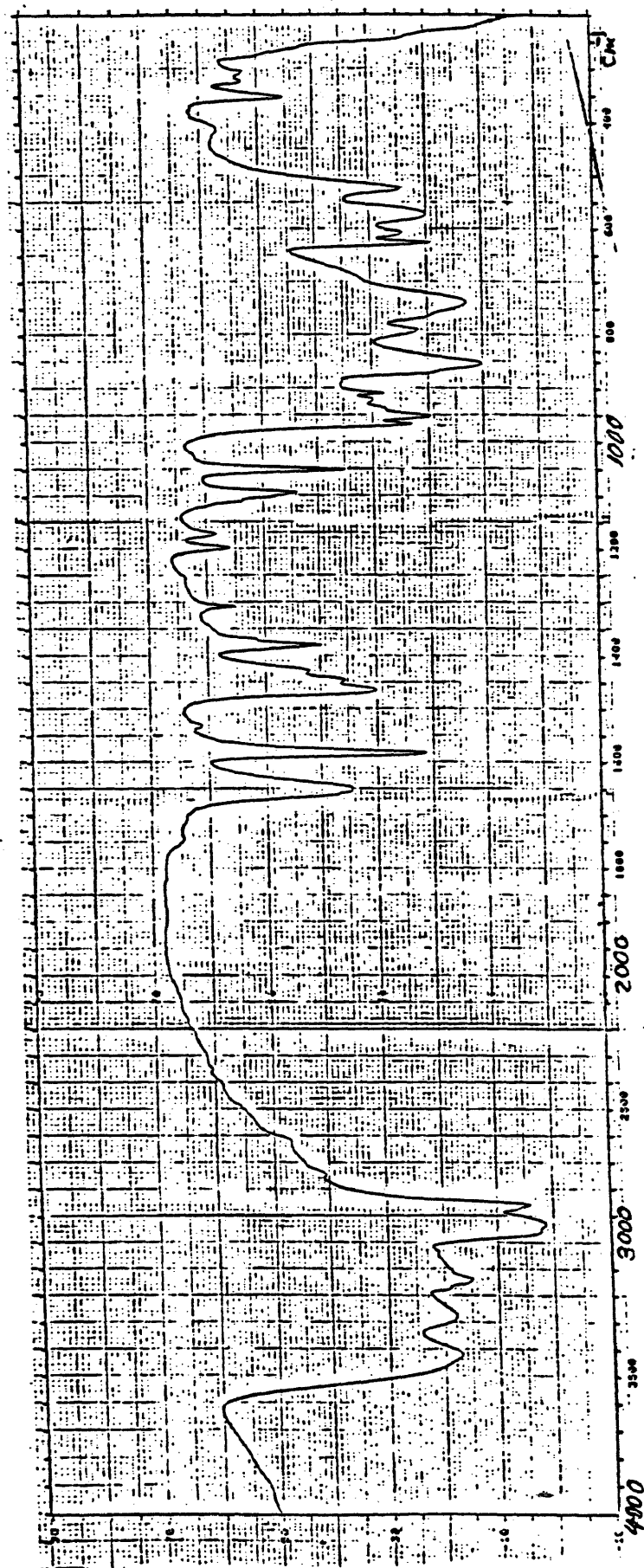


Figure 29. Infrared spectrum of $\text{MoO}(\text{O}_2)_2 \cdot \text{im} \cdot \text{H}_2\text{O}$ (Nujol mull).

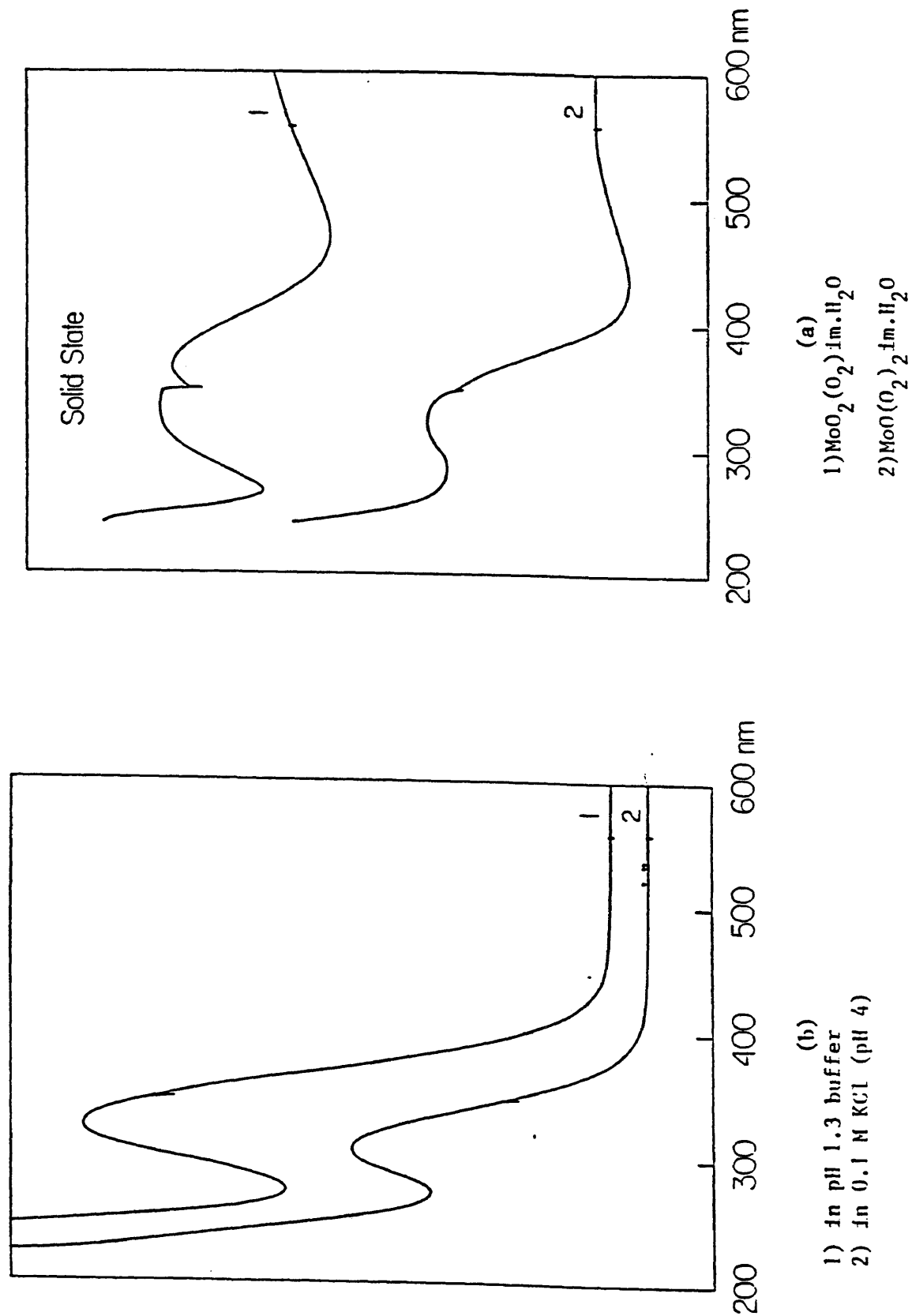


Figure 30. UV/visible spectra (a) Solid state spectra
(b) solution study of $\text{MoO}(\text{O}_2)_2 \cdot \text{im} \cdot \text{H}_2\text{O}$

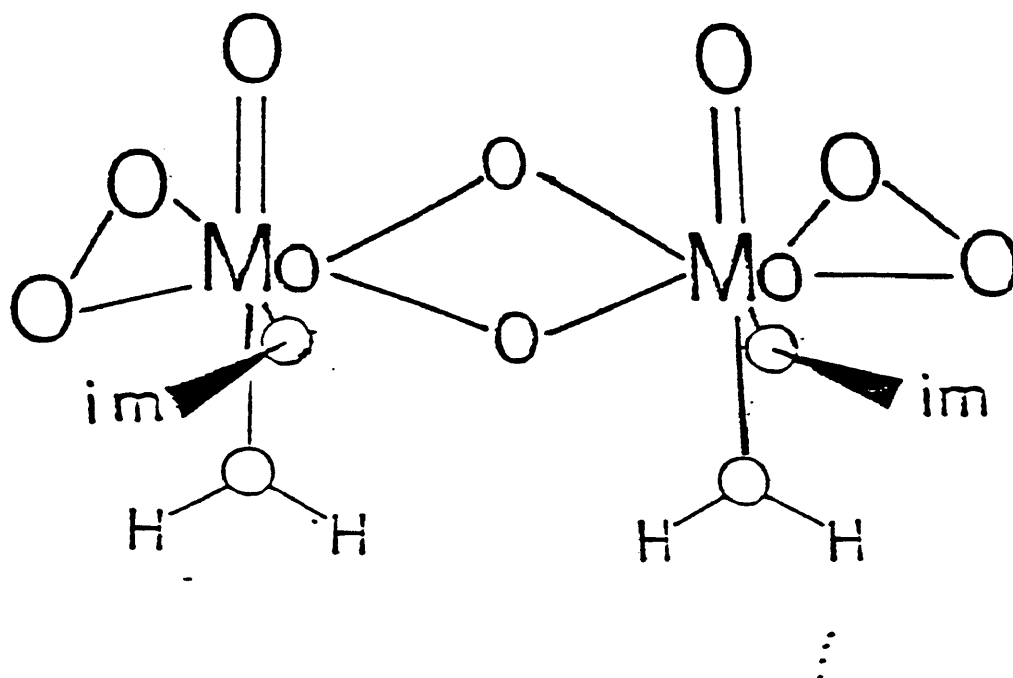


Figure 31. Possible structure of $\text{MoO}_2(\text{O}_2)\text{im} \cdot \text{H}_2\text{O}$

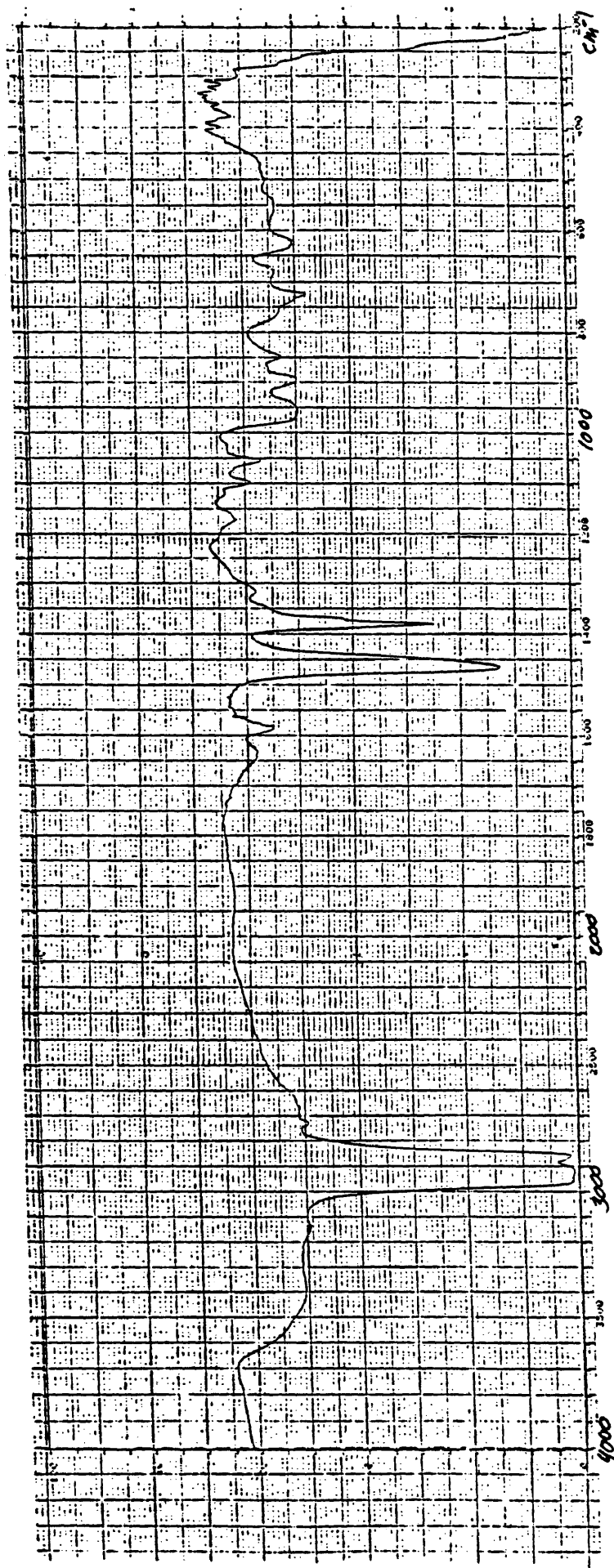


Figure 32. Infrared spectrum of $\text{MoO}_2(\text{O}_2) \cdot \text{H}_2\text{O}$ (solid state, Nujol mull)

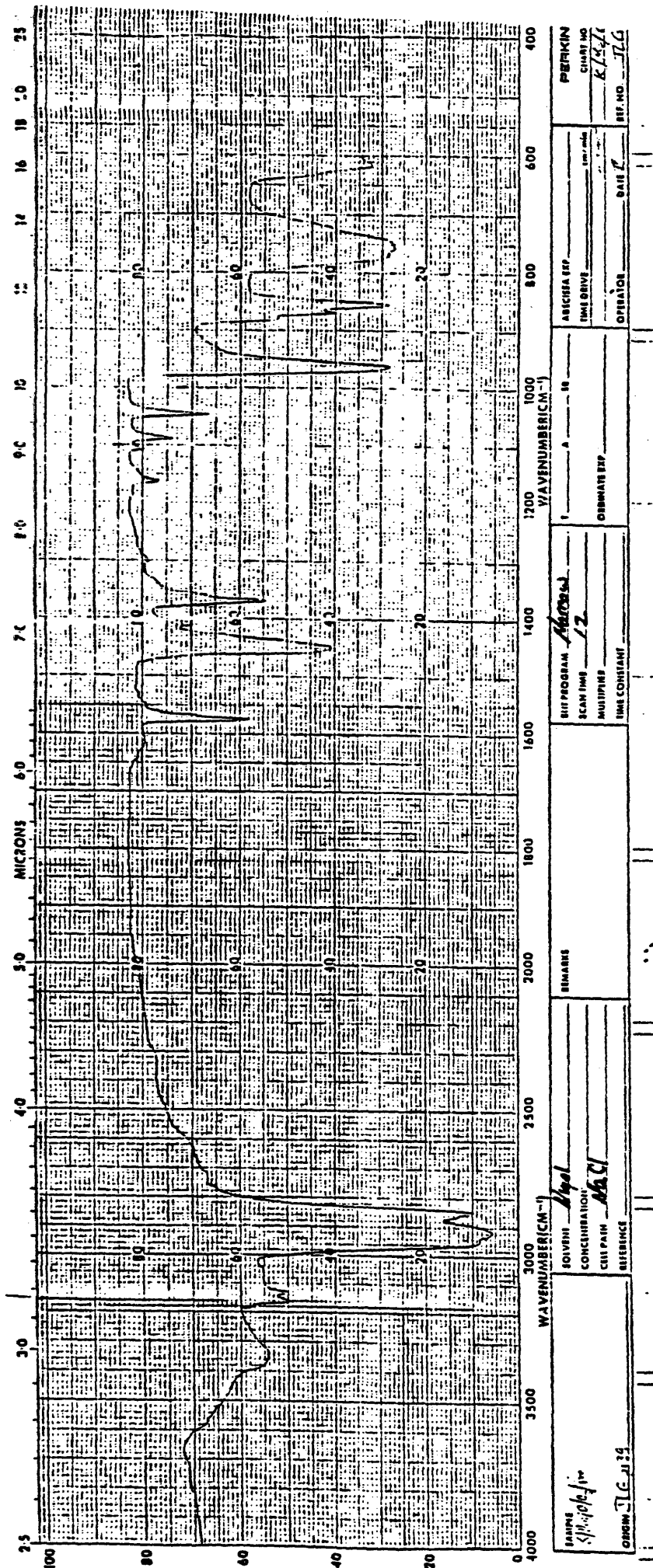


Figure 33. Infrared spectrum of precipitate from system K/Mo/O/O₂/im (Nujol mull)

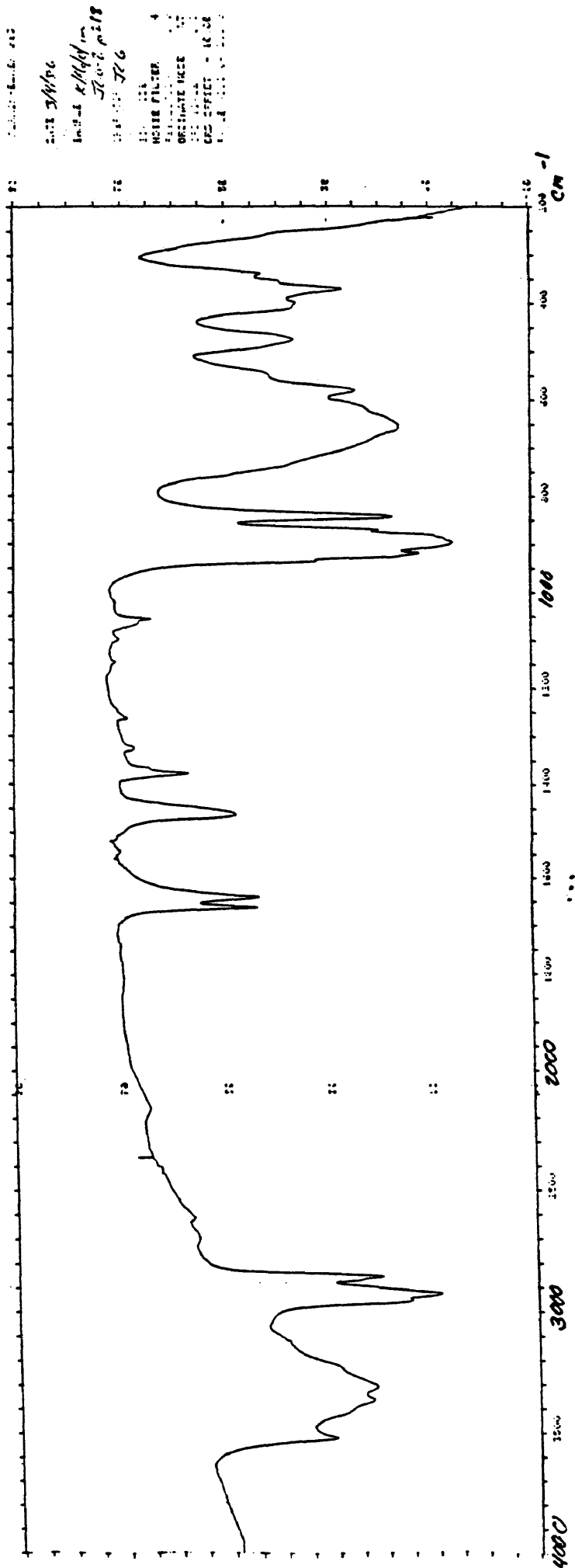


Figure 34. Infrared spectrum of precipitate from system K/Mo/O/1m (Nujol mull)

3.3 Peroxo oxalato molybdates

The pale yellow needlelike crystals obtained from the systems K/Mo/O/O_2 /im/asp and K/Mo/O/O_2 /asp were determined to be potassium oxodiperoxoxaltomolybdate(VI), $\text{K}_2[\text{MoO}(\text{O}_2)_2(\text{C}_2\text{O}_4)]$. The aspartic acid is apparently converted to oxalic acid which complexes with the molybdenum-peroxide in certain systems. The aqueous Mo(VI) system has also been found to catalyse the conversion of malic and malonic acids to oxalate- resulting in the formation of the same complex. When succinic acid is introduced to the Mo(VI) system though, no such conversion is observed. This is most likely due to the inability of succinic acid to form a five or six-membered intermediate ring system. Malic acid, malonic acid and aspartic acid can all form such rings. See figure 35. The mechanism for this conversion has yet to be elucidated but the work done so far indicates that for such a conversion an intermediate peroxoheteroligand molybdate sphere must be formed.

Initial characterization of the complex was made by comparison of the ir spectrum of the known compound with that obtained from the two systems reported here, K/Mo/O/O_2 /im/asp and K/Mo/O/O_2 /asp. See Fig. 36. The C=O stretchings appear as a very strong quartet at 1730, 1709, 1691 and 1673 cm^{-1} . The Mo=O stretch appears as another very strong peak at 976 cm^{-1} . The O-O stretching is present

as a strong peak at 868 cm^{-1} with a shoulder at 875 cm^{-1} .

Determination of the peroxide content proved to be more difficult than usual due to the oxidation of both peroxide and the oxalate by the Ce(IV) solution. Figure 37 shows a sample titration curve. The peroxide is oxidized first between 600 and 850 mv and the oxalate is then oxidized between 850 and 1150 mv. The compound contains between 20% and 25% oxalate. The wide range of values is due to the uncertainty involved in reading the curve.

An interesting phenomenon occurs with respect to the titration of peroxide in the compound. When the usual titration was carried out (20 to 40 minutes per 10 ml of Ce(IV) solution) the expected value of 19% to 20% peroxide was obtained. As longer titrations were run, the peroxide content seemed to decrease with increasing titration time. A 200 minute titration gave a value of 12.5% peroxide while a 60 minute run indicated that the compound contained 14.7% peroxide. This could be due to the fact that with the longer titrations, the compound spends a longer time in a highly acidic medium which may cause some decomposition of the compound before it is oxidized.

UV/visible spectra were run for the complex in solid state, in 0.1M KCl (pH 4) and in HCl/KCl buffer ($\mu=0.1$) at pH 1. The λ_{max} is often very hard to read due to the high signal to noise ratio. It is estimated to be 325 ± 10 nm. In 0.1M KCl it is 310 nm while at pH 1 the value is 325 nm.

Apparently the presence of imidazole is not necessary is the catalysis of aspartic acid to oxalate since the complex was also obtained from the system $\text{K/Mo/O/O}_2/\text{asp}$. The yield of $\text{K}_2[\text{MoO}(\text{O}_2)_2(\text{C}_2\text{O}_4)]$ was significantly lower without the imidazole in the system though. When imidazole was present the yield in the first crop was between 16% and 20%. Without it the yields are only 4% to 6%.

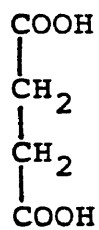
The temperature dependance of the reaction was then tested. The reaction of the system $\text{K/Mo/O/O}_2/\text{im/asp}$ was run following the same procedure as usual except that it was run on ice at 0°C . The $\text{MoO}_3/\text{H}_2\text{O}_2$ solution was added to the ligand solution and the precipitate formed without any further addition of H_2O_2 or additional heating. A small amount of dark yellow platelike crystals were obtained exclusively. Ce(IV) titration gave a peroxide content of 20% to 21% and no oxalate.

When the ligand solution was added to the $\text{MoO}_3/\text{H}_2\text{O}_2$ solution at 0°C a purple precipitate formed rapidly. A small amount was removed immediately, dried and washed with ethanol. The precipitate was then prepared as usual for an ir spectrum. On grinding most of the crystals decomposed rather violently, leaving a blueish/white residue that was most likely MoO_3 . The remaining purple precipitate showed no evidence of a ligand but did exhibit a strong peroxide stretch at 835 cm^{-1} . This indicated that the product was most likely a rather unstable tetra or triperoxo molybdenum

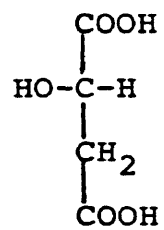
complex. The remaining purple crystals decomposed overnight in a dessicator to the same blueish/white molybdenum oxide.

The remaining solid that was in solution was placed in the refrigerator where it quickly and exothermically went back to a clear yellow solution of pH 5.8. A small crop of light yellow powder was obtained after one week. The ir spectrum indicated the presence of some ligand but no definite peroxide peak was observed. Ce(IV) titration confirmed the lack of peroxide. The infrared spectrum of the product appeared to be very similar to that of $K_2[MoO(O_2)_2(C_2O_4)]$ with the exception of the peroxide peak and the C=O quartet in the 1600 cm^{-1} region. In this product the quartet of bands that represented the C=O stretching was not as well resolved as that of $K_2[MoO(O_2)_2(C_2O_4)]$.

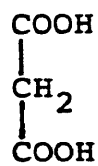
It would appear that the oxalate compound is formed only on heating. The effect of imidazole on the system has not yet been explained.



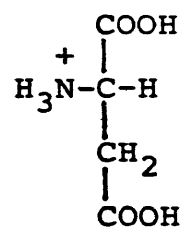
Succinic acid



Malic acid



Malonic acid



Aspartic acid

Figure 35.

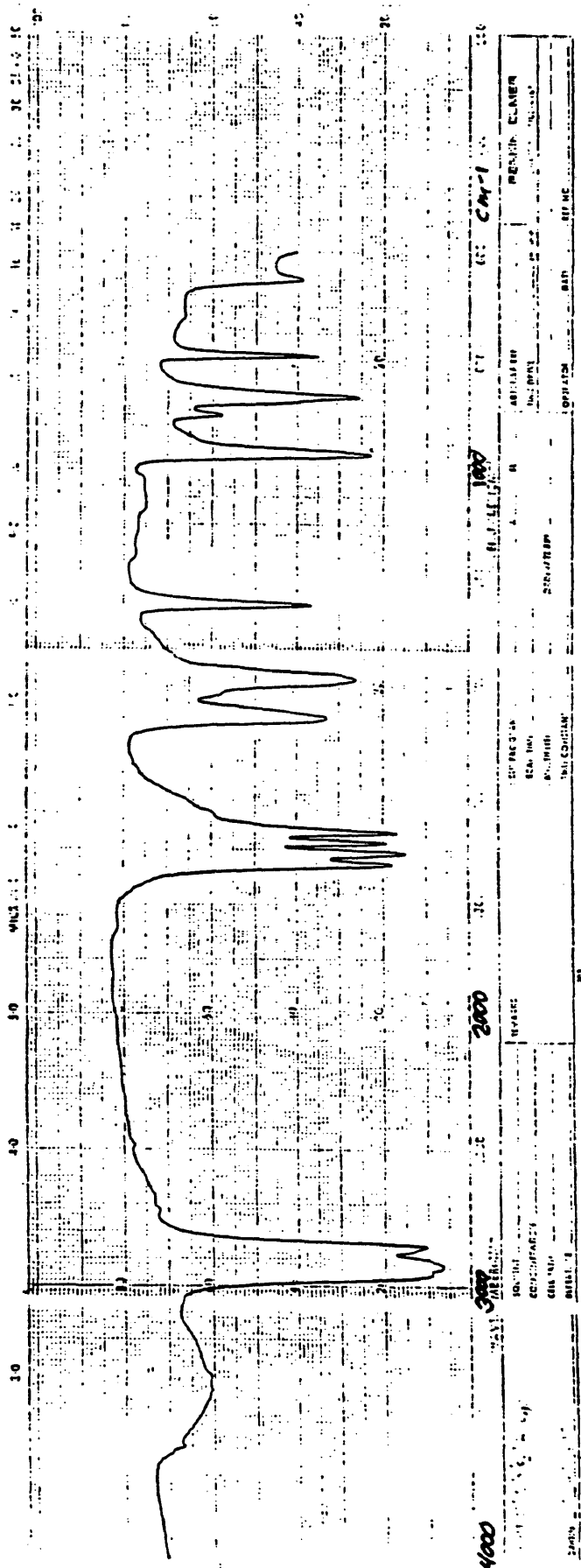


Figure 36. Infrared spectrum of $K_2[MoO(O_2)_2(C_2O_4)]$ (Nujol mull)

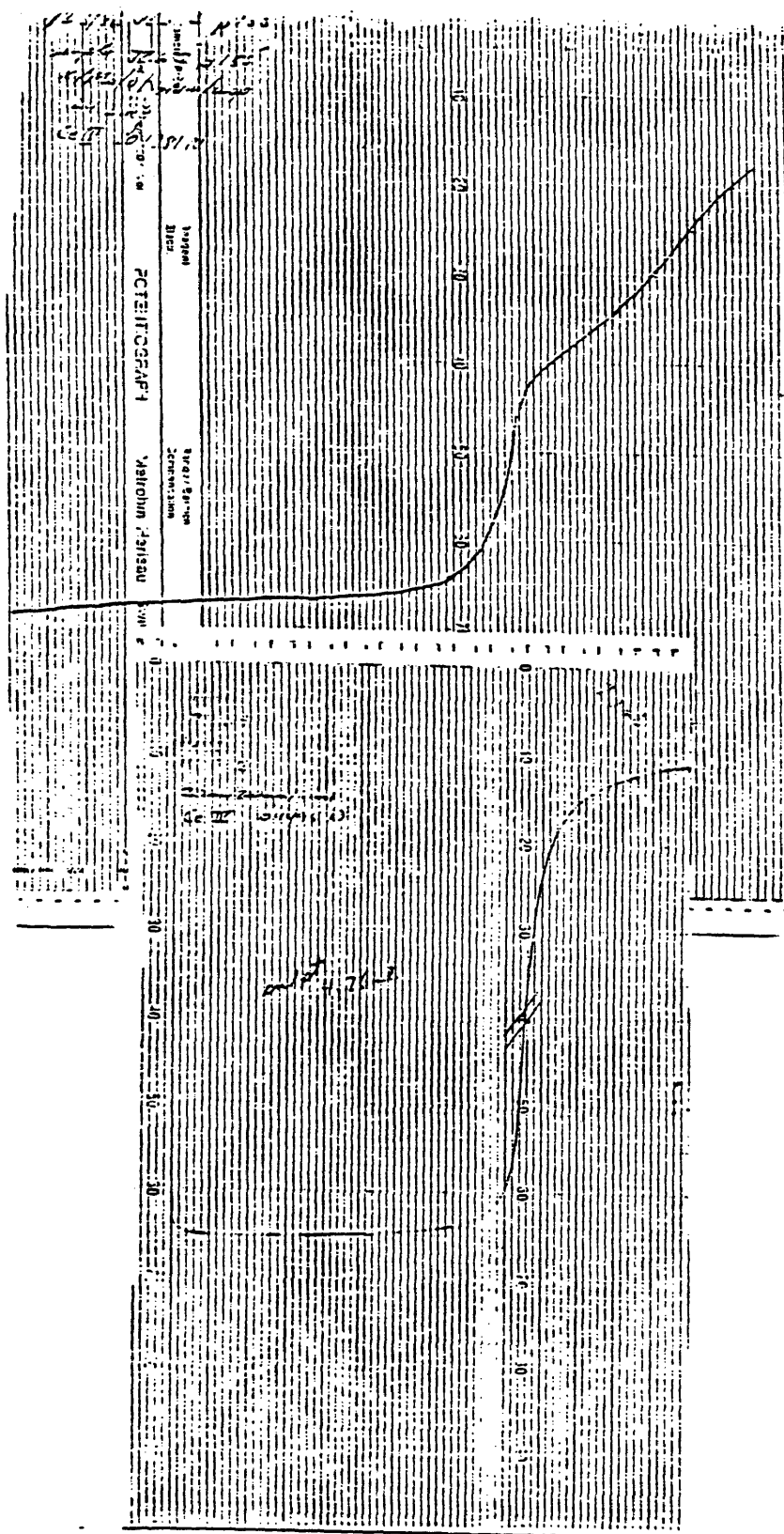


Figure 37. Typical Ce(IV) titration curves for $K_2[MoO(O_2)_2(ox)]$ (top) and $MoO(O_2)_2 \cdot im \cdot H_2O$ (bottom).

3.4 Peroxo histidine molybdates

The coordination of histidine is very often discussed in conjunction with that of imidazole since the R-group of histidine is the imidazole ring<45>. Aqueous complexes with histidine and Mo(VI) have been reported but no crystalline products were ever isolated<36>. One Mo(V)-his complex has been analyzed by x-ray structure analysis<63>. No oxoperoxohistidine complexes have been reported with Mo(VI).

We have, therefore, attempted to isolate oxoperoxohistidine molybdates(VI) from aqueous solutions of Mo(VI), H_2O_2 , histidine and a cation such as K^+ or NH_4^+ . To date no pure complex has been obtained but a mixture containing a possible complex with some peroxo molybdates has been obtained.

In most cases during research, yellow, irregularly shaped crystalline products were obtained from the various systems. The infrared spectra of these products indicated that most contained some peroxide but no ligand. Since no ligand was present the actual peroxide percentage was not determined. On other occasions a thick orange polymeric substance formed beneath yellow or orange-yellow solutions. Attempts to obtain crystals from these polymers proved unsuccessful.

The most successful attempt to isolate a complex came

from the system $\text{K/Mo/O/O}_2/\text{his}$ by the procedure that is outlined in 4.1.5.3. The calculations that were based on the formula, $\text{K}[\text{MoO}(\text{O}_2)_2\text{his}]\cdot\text{H}_2\text{O}$, gave theoretical values for the C, H and N content of 18.5%, 2.8%, and 10.8% respectively. Microanalysis of the product indicated that it contained only 2.7%C, 0.5% H and 1.0%N. These values are 14%, 21% and 9% of their respective theoretical values.

An inspection of the infrared spectrum of the product (fig.38) compared to that of histidine (fig. 39) shows a rather broad peak centered at 1640 cm^{-1} . This seems to correspond to the C=O stretch of histidine which appears as a stronger, sharper peak at 1635 cm^{-1} . The strong peak at 940 cm^{-1} is most likely due to the Mo=O stretch while the O-O stretch is represented by the peak at 857 cm^{-1} . Histidine, as the free base in the solid state, shows numerous absorptions between 1800 and 200 cm^{-1} while the product exhibits very few peaks in that region. The very weak peak at 1740 cm^{-1} in histidine remains unshifted in the product. Also unshifted in the product is the peak at 1378 cm^{-1} . The peak at 1593 cm^{-1} in the ligand now appears as a shoulder in the product at the same frequency due to the broadening of the C=O absorption.

In the region between 1300 cm^{-1} and 950 cm^{-1} the product exhibits no peaks though some overtones are evident. The three remaining strong peaks are located at 742 cm^{-1} , 616 cm^{-1} , and 576 cm^{-1} . They do not appear to

correspond exactly to any peaks in that region for histidine. They are most probably due to the coordination of the ligand to the metal. The broad absorptions between 3600 cm^{-1} and 3100 cm^{-1} are probably due to water of crystallization.

In the uv/visible range histidine exhibits no absorption between 900 nm and 200 nm in either the solid state or in 0.1M KCl at a concentration of 10^{-3} M. The product showed a λ_{max} at 350 nm for the solid state nujol mull. In a solution of 0.1M KCl at pH 5.3 a λ_{max} of 310 was observed while at pH 1 in an HCl/KCl buffer the λ_{max} was 320 nm.

When the procedure of the reaction was altered, less promising products were obtained. If the ratio of the molybdenum to histidine is reduced to one to one a yellow precipitate forms immediately after the addition of the $\text{MoO}_3/\text{H}_2\text{O}_2$ solution to the KOH/histidine solution. The Ce(IV) titrations of these products gave values of 5 to 10% peroxide but the ir spectra indicated that little or no ligand was present. Adding the his/KOH solution to the $\text{MoO}_3/\text{H}_2\text{O}_2$ solution yielded similar results.

While much of the reported data seems to indicate that the product is a complex, the microanalysis gives even greater proof that it is not. Calculating the theoretical peroxide content also indicates that the product is most likely a mixture. For the proposed formula the peroxide

content should be 16.5% but the experimental data gave values between 18% and 22%. This higher than expected value could be due to the peroxy-molybdate salts in the mixture that would have higher peroxide percentages, by weight.

Though it seems that a pure complex has not yet been isolated, the preliminary results look quite promising. Further study as well as modifications of the procedure are necessary to obtain the intended pure complex.

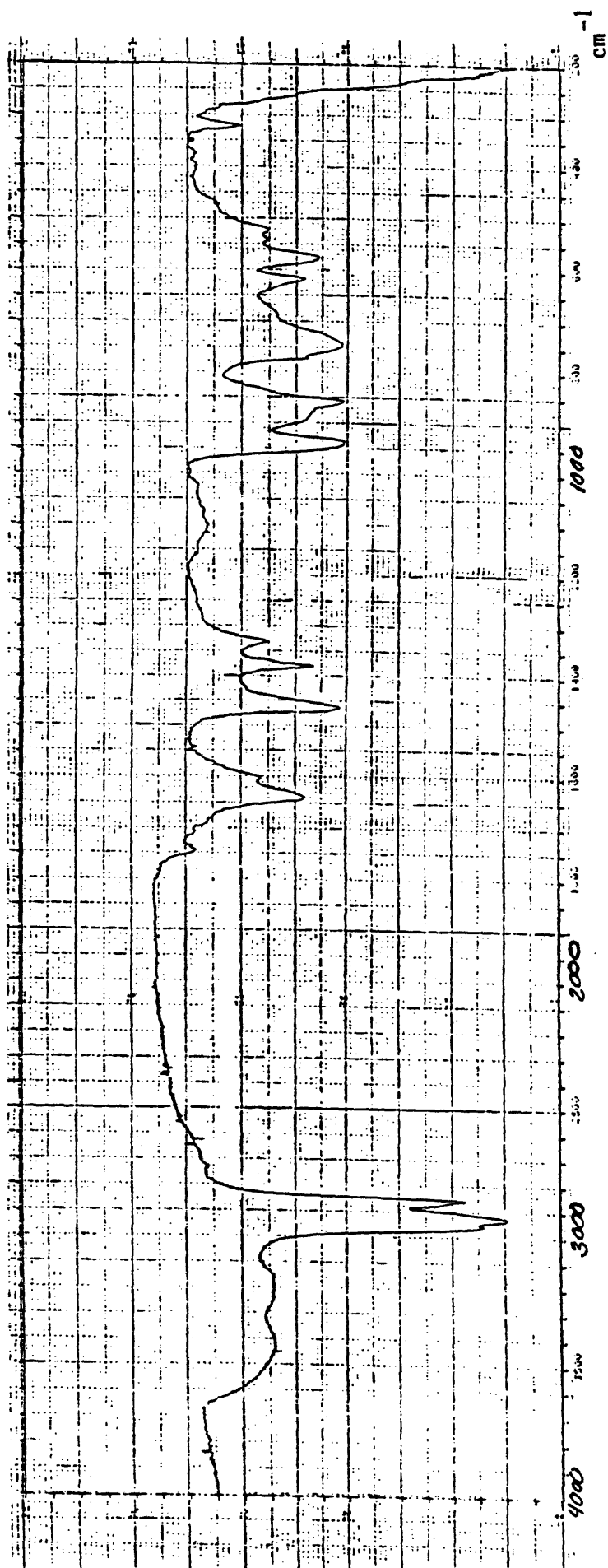


Figure 39. Infrared spectrum of the precipitate from the system K/Mo/O/O₂/his. (Nujol mull)

Table 7
Results of analysis of compounds and other products

Compound (or system)	% found				% calculated			
	C	H	N	O ₂ ²⁻ avg.	C	H	N	O ₂ ²⁻
MoO(O ₂) ₂ ·1m·H ₂ O	13.45	2.55	10.45	20	13.7	2.3	10.7	24.4
MoO ₂ (O ₂) _{1m} ·H ₂ O	12.50	2.10	9.65	14	14.6	2.4	11.0	13.0
K ₂ MoO(O ₂) ₂ (C ₂ O ₄)	7.10	0.19	0.27	19	7.0	0.5	0.0	17.7
K/Mo/O/O ₂ /1m	7.81	1.11	5.96	20	12.0	1.0	9.3	21.3
K/Mo/O/1m	2.58	0.89	1.83	--	16.0	3.0	12.0	--
NH ₄ /Mo/O/O ₂ /1m	2.74	2.80	9.08	23	13	3	15	22.8
K/Mo/O/O ₂ /h1s	2.65	0.55	1.05	20	19.5	2.4	11.5	17.6

4 Experimental

4.1 Preparation of the compounds

4.1.1 Vanadium-imidazole system

4.1.1.1 System K/V/O/O₂/im

The preparation of a complex from this system has been attempted by five different procedures, though none were successful. A summary of the procedures is given below:

a) KOH(.56g,10 mmole) and V₂O₅(.91g,10 mmole V) are stirred together in deionized water(5 ml). H₂O₂(30%, 1 ml,9 mmole) is added slowly with a dropping pipet. The resulting solution is placed in an ice bath and additional H₂O₂(30%,5 ml,45 mmole) is added in the same manner. Imidazole(.68g,10 mmole) is dissolved in deionized water(2 ml) and is added dropwise. The clear yellow solution (pH 5) is stirred for 30 minutes in the ice bath, then for 2 hours at room temperature. It is then heated (30-40°C) for 30 minutes with continued stirring. No precipitate forms and the solution is covered and set aside. After 3-4 days the solution turns brown indicating a reduction of V(V) to V(IV). A very small amount of brown solid forms at pH 7 and is discarded as V(IV).

b) V_2O_5 (.91g, 10 mmole V), KOH (1.0M, 10ml, 10 mmole) and imidazole (.68g, 10 mmole) are stirred together at room temperature. H_2O_2 (30%, 15 ml, 135 mmole) is added very slowly with a dropping pipet. The final pH is 5-6. Concentrated HCl is added to reduce the pH to 4. The next day, ethanol (95%) is used to induce precipitation. IR spectrum indicates that no ligand is present.

c) Imidazole (.68g, 10 mmole) is dissolved in water (5 ml). V_2O_5 (.91g, 10 mmole V) is added with stirring. H_2O_2 (30%, 5 ml, 45 mmole) is added slowly with a dropping pipet. Maximum temperature of the reaction mixture is 40-45°C. pH of the final solution is 4. The solution is placed on ice and solid KCl (.83g, 11 mmole) is added with stirring. An additional 2 ml of H_2O_2 (30%, 18 mmole) is added. Stirring is continued for one hour. The solution is covered and placed in the refrigerator where it turns green. A green, V(IV), precipitate is obtained.

d) Imidazole (.68g, 10 mmole) is dissolved in KOH (1.0M, 10 ml, 10 mmole). Solid V_2O_5 (.91g, 10 mmole V) is added and stirred until dissolved. H_2O_2 (30%, 10 ml, 90 mmole) is added slowly with rapid stirring. The reaction is slightly exothermic with a final pH of 6. Stirring is continued for 30 minutes-being heated at 50°C for the final 15 minutes. Ethanol is used to obtain a precipitate. IR spectrum showed no ligand was present.

e) V_2O_5 (.91g, 10 mmole V) is dissolved in KOH (1.0M, 15

ml, 15 mmole) with slight heating. H_2O_2 (30%, 1.5 ml, 15 mmole) is added to the clear warm solution. The resulting yellow-orange solution is placed on ice and stirred slowly while more H_2O_2 (30%, 5 ml, 45 mmole) is added. Imidazole (.68g, 10 mmole) is dissolved in water (2 ml) and is added over one-half minute. Stirring is continued for 30 minutes at room temperature. The solution is then covered and placed in an ice bath for one hour. H_2O_2 (30%, 3 ml, 27 mmole) is stirred in and the pH is fixed to 6 with HCl (2N). After 24 hours ethanol (95%) is used to induce precipitation. The IR spectrum indicated that no ligand was present.

4.1.1.2 System V/O/O₂/im

The preparation of a complex in this system has been attempted by three different procedures. In some cases, small amounts of KOH or HCl were used to fix the pH. A summary of these attempts is given below:

a) V_2O_5 (.91g, 10 mmole V) is dissolved in H_2O_2 (30%, 15 ml, 135 mmole) with stirring on ice. This reaction vigorously produces gases. Imidazole (.68g, 10 mmole) is dissolved in water (2 ml) and is added slowly with a dropping pipet when the reaction of the V_2O_5 and H_2O_2 is nearly complete. The resulting cloudy, yellow-orange solution has a pH of 2-3. Saturated KOH (4-6 drops) is

added to pH 4. Stirring is continued on ice for one hour. The solution is then covered and set aside overnight. Ethanol (95%) is used to induce precipitation. The precipitate is filtered and washed with ethanol (50% and 95%). IR spectrum showed no ligand was present.

b) Imidazole (.68g, 10 mmole) is dissolved in deionized water (10 ml). V_2O_5 (.91g, 10 mmole V) is added and the mixture is stirred for 2-3 minutes. Not all of the V_2O_5 dissolves. H_2O_2 (30%, 2 ml, 18 mmole) is added slowly. The solution is placed in an ice bath and an additional 8 ml (72 mmole) of H_2O_2 is added. Stirring is continued for one hour. The pH is raised from 3 to 4 with KOH (1.0M). The solution is covered and left overnight. It is then stirred for one hour at room temperature and for another hour at 50° C. A small amount of brown-yellow precipitate forms beneath a red-orange solution at pH 5-6. The precipitate is filtered and washed with ethanol (95%).

c) V_2O_5 (.91g, 10 mmole V) and imidazole (1.36g, 20 mmole) are vigorously stirred in water (10 ml) for two minutes in an ice bath. H_2O_2 (30%, 12 ml, 108 mmole) is added slowly over about one minute with continued rapid stirring on ice. The clear yellow solution has a pH of 6. Stirring is continued for two hours. An additional 4 ml of H_2O_2 (30%, 32 mmole) is added. The ice bath is then removed and the solution is stirred at 50° C for 30 minutes. Red platelike crystals form beneath a red orange solution (pH 6)

after about one week. The crystals are filtered and washed with 50% and 95% ethanol. The IR spectrum indicated the possible presence of a ligand but Ce(IV) titration showed no trace of peroxide.

4.1.2 Molybdenum- imidazole system

4.1.2.1 System K/Mo/O/im

MoO_3 (1.44g, 10 mmole) is added to KOH (1.0M, 10 ml, 10 mmole) and the mixture is stirred at 50-60°C. After about 5-10 minutes, the mixture becomes very thick and white with stirring almost impossible. Imidazole (1.36g, 20 mmole) is dissolved in deionized water (5 ml) and is added dropwise to the MoO_3 -KOH mixture. The solid begins to dissolve as the imidazole solution is added. Heating and stirring are maintained until a clear solution is obtained and then for an additional 15 minutes. The pH is about 7. The solution is left uncovered and allowed to slowly evaporate. Clear prism-like crystals form within 24 hours. The crystals are filtered and washed twice with small amounts of cold, deionized water and are air dried. They are analyzed by infra- red spectrum.

Observations

1) When equimolar amounts of MoO_3 and imidazole are used, a mixture of precipitates is obtained.

2) Washing the crystals with ethanol or acetone seems to disrupt the integrity of the crystals, while washing with water does not. This indicates that the crystals are most likely hydrated.

3) Crystals can also be obtained more rapidly by evaporating at 60-65° C without stirring. The crystals generally tend to be smaller though.

4.1.2.2 $\text{MoO}(\text{O})_2 \cdot \text{im.H}_2\text{O}$

MoO_3 (1.44g, 10 mmole) is dissolved in H_2O_2 (30%, 10 ml, 10 mmole) under stirring at 45-50° C for 3-4 hours (or overnight at room temperature) until a clear yellow solution is obtained. Any undissolved material is filtered off and the solution is cooled to room temperature. Imidazole (.68g, 10 mmole) is dissolved in deionized water (2-3 ml) and is added, dropwise, to the slowly stirring $\text{MoO}_3/\text{H}_2\text{O}_2$ solution. As each drop is added, the solution becomes partly dark red-brown then returns to yellow within a few seconds. The next drop of imidazole should not be added until the solution is completely yellow. As the last few drops are added, the solution will remain red-brown. Addition should be continued at the same rate. Slow stirring is continued for 1-2 hours as the solution gradually returns to yellow. The solution is covered and set aside. Within 1-2 days large prism-like crystals form beneath a yellow solution of pH 4-5. The crystals are vacuum filtered and washed with 50% and 95% ethanol and dried over Drierite before analysis.

Observations

1) Leaving the crystals in the mother liquor for several days results in the breakdown of the crystal-leaving a yellow polymeric substance which could not be analysed by IR using a Nujol mull.

2) The age of the $\text{MoO}_3/\text{H}_2\text{O}_2$ solution does not seem to affect the outcome of the reaction .

3) The reaction is sometimes quite exothermic, with a maximum temperature of 105°C and a rapid evolution of gases. In most cases, the maximum temperature does not exceed 50°C with slower bubbling.

4.1.2.3 $\text{MoO}_2(\text{O}_2)\text{im.H}_2\text{O}$

The $\text{MoO}_3/\text{H}_2\text{O}_2$ solution is prepared in the same manner as given above in $\text{MoO}(\text{O}_2)_2\text{im}$. Imidazole(.68g, 10 mmole) is dissolved in deionized water(2-3 ml) and is added all at once to the slowly stirring $\text{MoO}_3/\text{H}_2\text{O}_2$ solution. The resulting solution is stirring for 15 minutes and is then covered and set aside. Yellow needle-like crystals form beneath a yellow solution within 1-2 days and are filtered and washed with 50% and 95% ethanol and dried over Drierite before analysis. A second crop of smaller needle-like crystals precipitates in the filtrate almost immediately after filtration of the first crop. They are filtered, washed and dried in the same manner as the first crop.

Both crops are then analysed.

Observations

1) The second crop is generally produced in a much higher yield than the first.

2) Three different things can happen after the imidazole is added. The resulting solution may become dark red-brown and return to yellow vigorously and exothermically (maximum temperature is 105°C) within 1-2 minutes. It may become dark red-brown and return to yellow gradually with a maximum temperature of $30-35^{\circ}\text{C}$. Or, it may remain yellow with no temperature change. This usually happens when the $\text{MoO}_3/\text{H}_2\text{O}$ solution is 3-4 weeks old.

3) The age of the solution does not seem to affect the final outcome of the reaction- except as stated in 2.

4.1.2.4 System $\text{NH}_4/\text{Mo}/\text{O}/\text{O}_2/\text{im}$

$(\text{NH}_4)_2\text{MoO}_4$ (1.96g, 10 mmole) is dissolved in H_2O_2 (30%, 10 ml, 90 mmole) with stirring. Imidazole (.68g, 10 mmole) is dissolved in deionized water (2 ml) and added slowly. The reaction mixture turns deep red-brown and is placed in an ice bath where stirring is continued for 30 minutes when a precipitate forms. Stirring is continued for another 30 minutes. The small yellow crystals are filtered and washed with ethanol (95%) and dried over Drierite before analysis.

4.1.2.5 System K/Mo/O/O₂/im

MoO₃ (1.44 g, 10 mmole) is dissolved in H₂O₂ (30%, 10 ml, 10 mmole) as described in 4.1.2.2. Imidazole (.34g, 5 mmole) is dissolved in deionized water (2 ml) and is added slowly to the slowly stirring MoO₃/H₂O₂ solution. There is no permanent color change though the solution does become slightly red-brown with each addition of imidazole, as in previous reactions. There is also no temperature increase.

Saturated KOH is then added dropwise to the yellow solution until a pH of 6 is achieved. At this point, the solution remains a dark red-brown and gives off gases slightly exothermically with a maximum temperature of 40°C. After 30 minutes of stirring, a precipitate forms beneath a slightly red-orange solution at pH 5. The solution is set aside for further precipitation. The yellow precipitate is filtered, washed with ethanol (95%) and dried over Drierite before analysis.

Observations

1) If the pH is raised above 6, the maximum temperature increases to 100°C, accompanied by a rapid change to yellow and a vigorous release of gases. The result is a peroxymolybdate precipitate with no ligand.

4.1.3 Molybdenum-imidazole-aspartic acid system

4.1.3.1 $K_2[MoO(O_2)_2(C_2O_4)]$

KOH (1.40g, 25 mmole) is dissolved in deionized water(5 ml). Aspartic acid(1.33g, 10 mmole) is then added and stirred until dissolved. Imidazole(.68g, 10 mmole) is then added to the solution and dissolved. MoO_3 (1.44g, 10 mmole) is stirred together with H_2O_2 (30%, 10ml, 90 mmole) until a clear yellow solution is obtained. Any undissolved MoO_3 is filtered out. The MoO_3/H_2O_2 solution is slowly added to the ligand solution. The resulting solution quickly turns dark red-brown. After about 1-2 ml of the MoO_3/H_2O_2 solution is added the reaction solution begins to evolve gases very exothermically while turning yellow. The remaining MoO_3/H_2O_2 is added at such a rate to keep the evolution of gases to a minimum. The final clear yellow solution is covered and set aside overnight. The pH is 5.5-6.

The next day the solution is heated to 60-70° C and stirred until a precipitate begins to form(1-1 1/2 hours). H_2O_2 (30%, 3-4 ml) is added and the solution is stirred until it again becomes clear. The solution is removed from the heat, covered and set aside. Pale yellow needle-like crystals form within 2 hours beneath a yellow solution of pH 5-6. They are filtered and washed with 50% and 95%

ethanol and dried over Drierite before analysis.

Observations

1) If the crystals are not filtered within 24 hours, another dark yellow precipitate forms along the bottom and sides of the glass beaker. These plate-like crystals are filtered and washed with 50% and 95% ethanol separately, or are separated with great difficulty later. They are also dried over Drierite before analysis.

4.1.4 Molybdenum-aspartic acid system

4.1.4.1 $K_2 [MoO(O_2)_2 (C_2O_4)]$

MoO_3 (1.44g, 10 mmole) is dissolved in H_2O_2 (30%, 10 ml, 10 mmole) as in 4.1.2.2. KOH (1.40g, 25 mmole) is dissolved in deionized water (5 ml). Aspartic acid (1.33g, 10 mole) is added to the KOH solution and stirred until dissolved. The $MoO_3 / H_2 O_2$ solution is added dropwise to the slowly stirring ligand solution. After about 1 ml of the solution is added, the resulting red-brown reaction solution begins to vigorously and exothermically evolve gases while turning yellow. The remaining $MoO_3 / H_2 O_2$ solution is added at a rate that keeps the bubbling to a minimum. After the final addition, the solution is covered and set aside. Pale yellow needle-like crystals form within 24 hours beneath a yellow solution of pH 4.6-4.9. They are filtered, washed with 50% and 95% ethanol and dried over Drierite before analysis.

Observations

1) Unlike the $K/Mo/O/O_2/asp/im$ system that had also produced $K_2 [MoO(O_2)_2 (C_2 O_4)]$ no additional heating or $H_2 O_2$ is required to obtain a precipitate.

2) The yield of $K_2 [MoO(O_2)_2 (C_2 O_4)]$ is substantially lower in this system with regard to $K/Mo/O/O_2/asp/im$.

4.1.5 Molybdenum-histidine system

4.1.5.1 System Mo/O/O₂/his

The preparation of a compound in this system has been attempted by three different methods. A summary of the procedures is given below:

a) MoO₃ (1.44g, 10 mmole) is dissolved in H₂O₂ (30%, 10 ml, 90 mmole) as in 4.1.2.2. Solid histidine (1.55g, 10 mmole) is added slowly and stirred until dissolved (about 30 minutes). The resulting yellow solution is covered and set aside. A thick orange polymeric precipitate forms within 2-3 days at a pH of 3.5-3.7. If no precipitate forms, the solution is heated at 45° C for 10 minutes until a precipitate forms. The product is filtered and washed with ethanol (95%) and dried over Drierite before analysis.

b) MoO₃ (1.44g, 10 mmole) is dissolved in H₂O₂ (30%, 10 ml, 90 mmole) as in 4.1.2.2 and heated to 55-60° C. Solid histidine (1.55g, 10 mmole) is added rapidly. The reaction is vigorous and exothermic with a rapid color change from yellow to red-brown then back to yellow accompanied by a vigorous release of gases. A precipitate forms shortly without any additional heating at a pH of 3.5-4. The yellow precipitate is filtered, washed with ethanol (95%) and dried over Drierite before analysis.

c) Histidine (1.55g, 10 mmole) is dissolved in deionized

water (10 ml) at 70-80° C. MoO_3 (1.44g, 10 mmole) is dissolved in H_2O_2 (30%, 10 ml, 90 mmole) as in 4.1.2.2. The hot histidine solution is added all at once to the $\text{MoO}_3/\text{H}_2\text{O}_2$ solution with slow stirring. The reaction is vigorous and exothermic with a rapid release of gases and a rapid color change from yellow to red-brown and back to yellow. If no precipitate forms within 2 days, the solution is heated to 75°C for 15 minutes until a precipitate forms. The resulting yellow precipitate is filtered and washed with 95% ethanol, dried over Drierite and analysed.

4.1.5.2 System $\text{NH}_4/\text{Mo}/\text{O}/\text{O}_2/\text{his}$

$(\text{NH}_4)_2\text{MoO}_4$ (1.96g, 10 mmole) is dissolved in H_2O_2 (30%, 10 ml, 10 mmole) with stirring for 1 minute. Solid histidine (1.55g, 10 mmole) is added slowly with continued stirring. As the histidine dissolves the solution turns dark red-brown then bubbles vigorously and exothermically as it changes to yellow orange. A precipitate forms overnight and is filtered and washed with 95% ethanol and dried over Drierite before the yellow crystals are analysed.

Observations

1) If no precipitate forms spontaneously, heating will only polymerize the reaction mixture. This tends to happen

when the $(\text{NH}_4)_2\text{MoO}_4/\text{H}_2\text{O}$ solution is not freshly made.

4.1.5.3 System K/Mo/O/O₂/his

Histidine(1.55g, 10 mmole) is dissolved in KOH(1.0M, 11 ml, 11 mmole) with stirring at room temperature. MoO₃ (2.88g, 20 mmole) is dissolved in H₂ O₂ (30%, 20 ml, 180 mmole) as in section 4.1.2.2 and is added dropwise, slowly, to the moderately stirring ligand solution. The resulting solution quickly turns red-brown and bubbles slightly. After about 3-5 ml of the MoO₃/H₂O₂ solution has been added, the solution vigorously and exothermically turns yellow with a rapid evolution of gases. Exothermic bubbling continues for the remainder of the addition. The solution is cooled to room temperature or overnight. Saturated KOH is added slowly with stirring to the yellow solution to raise the pH from 2 to about 7.6 where it again turns and remains red-brown. A few more drops of KOH are added until the solution begins to bubble. It then quickly and exothermically turns yellow again. Stirring is continued for 10-20 minutes or until a precipitate begins to form.

The solution is covered and set aside for further precipitation. The small yellow crystals are filtered, washed with 50% and 95% ethanol and dried over Drierite before analysis.

4.2 Physical measurements of the compounds

4.2.1 Infrared spectra of the complexes

4.2.1.1 Nujol mulls

The infrared spectra of the compounds were recorded in Nujol mulls on NaCl or CsBr plates using the Perkin-Elmer model #1320 and #983 spectrophotometers.

Procedure:

A small amount of the sample (5-10 mg) is finely ground with a mortar and pestle. One drop of Nujol is added to make a smooth mull. The mull is smeared on the salt plate and is placed in the sample holder in the spectrophotometer. The spectrum is obtained in the wavelength range of 4000 cm^{-1} to 600 cm^{-1} for mulls on the NaCl plates and 4000 cm^{-1} to 200 cm^{-1} for mulls on the CsBr plates.

4.2.1.2 Hexachlorobutadiene (HCBd) mulls

Nujol absorbs between 3000 cm^{-1} and 2800 cm^{-1} and between 1500 cm^{-1} and 1350 cm^{-1} in the infrared region while HCBd absorbs between 1650 cm^{-1} and 1500 cm^{-1} , 1250 cm^{-1} and 1150 cm^{-1} and 1025 cm^{-1} and 750 cm^{-1} [81]. HCBd is transparent in the regions where Nujol absorbs. It is therefore often used in obtaining spectral information obscured by Nujol. The procedure for preparing the HCBd mull is essentially the same as the Nujol mull. The sample is finely ground and a

drop of HCBD is added to make a smooth mull. The mull is smeared on NaCl plates. The spectrum is recorded between 4000 cm^{-1} and 1250 cm^{-1} .

4.2.2 UV/visible Spectra

The UV/visible spectra are recorded on the Brinkman Acta MVI spectrophotometer using a 1 cm quartz cuvette for solutions and polyethylene plates for solids.

Procedure for solutions:

About 20 mg of the complex is dissolved in HCl/KCl buffer (50 ml, $\mu=0.1$) in the pH range of 1. The spectrum is scanned from 900 nm to 200 nm. The λ_{max} is measured. An analogous spectrum is recorded for the compound in KCl (0.1M, 50 ml)

Procedure for solids:

A small amount of the solid is finely ground with a mortar and pestle. A drop of Nujol is added to make a smooth mull. The mull is smeared on a polyethylene plate and placed in the sample holder of the spectrophotometer. The spectrum is recorded from 900 nm to 200 nm and the λ_{max} is measured.

4.3 Analysis of the complexes

4.3.1 Analysis for peroxide

4.3.1.1 Ce(IV) Potentiometric titration

Ce(IV) is a very good oxidizing agent that is stable for several years in sulfuric acid solutions. It is reduced exclusively from Ce(IV) to Ce(III) in acidic media.(3,4) It reacts with peroxide in the following manner:



The peroxide content of the compound can thus be determined. The Ce(IV) solution is prepared by dissolving ceric ammonium sulfate in a dilute sulfuric acid solution to obtain a 0.04XX N Ce(IV) solution. This is then standardized against a potassium ferrocyanide solution of known normality by titrating a known amount of the $\text{K}_4\text{Fe(CN)}_6$ solution with the Ce(IV) solution. The normality is then calculated from the known equivalents of $\text{K}_4\text{Fe(CN)}_6$ titrated and the endpoint<84>. The titrations were carried out on the Brinkman Potentiograph model # E536 and the Metrohm Dosimat model # 986. The procedure for peroxide determination with Ce(IV) solution is given below:

20-30 mg of the compound is dissolved in H_2SO_4 (2N, 8 ml) and is then diluted with deionized water (8 ml). The sample is titrated versus a standardized Ce(IV) solution

$((\text{NH}_4)_2 \text{Ce}(\text{SO}_4)_6 \cdot 2\text{H}_2\text{O}$ in H_2SO_4). The equivalence point is determined and the peroxide content of the compound can be determined.

4.3.2 Analysis for C,H and N

The C,H and N analyses were done by microanalysis at Atlantic Microlab Inc, Atlanta, Ga.

4.3.3 Molybdenum analysis

The molybdenum content of the compounds is being determined at Galbraith Laboratories Inc. Knoxville, Tenn.

4.3.4 X-ray structure analysis

The x-ray structure analysis of the complexes is in progress, carried out by Professor Ekk Sinn at the University of Virginia in Charlottesville.

Conclusions

Molybdenum, the heaviest trace metal essential for life, serves as a cofactor to many enzymes and probably has many other functions not yet known. Imidazole, histidine and peroxide are also very important as bioligands. Our goal has been to synthesize and characterize complexes involving Mo(VI) and these ligands.

Our studies of Mo(VI)-peroxo systems with imidazole, histidine and aspartic acid have yielded some interesting results. The two crystalline complexes of the forms $\text{MoO}(\text{O}_2)_2 \cdot \text{im} \cdot \text{H}_2\text{O}$ and $\text{MoO}_2(\text{O}_2) \cdot \text{im} \cdot \text{H}_2\text{O}$ were obtained from the Mo(VI)-peroxo-imidazole system. They exhibit vastly different characteristics including decomposition point, physical appearance, peroxide content and infrared spectrum, yet their preparation procedures are strikingly similar. $\text{MoO}(\text{O}_2)_2 \cdot \text{im} \cdot \text{H}_2\text{O}$ appears to be slightly more stable than the monoperoxo complex in that it can be produced more readily, in higher yields, while $\text{MoO}_2(\text{O}_2) \cdot \text{im} \cdot \text{H}_2\text{O}$ is rather hard to obtain, even in low yields. The results of x-ray structure analysis may give some insight into this area but more studies are no doubt necessary to understand the mechanism of each complex's formation.

The discovery that the Mo(VI)-peroxo system catalyses the conversion of aspartate to oxalate may help in

elucidating the mechanism where other organic acids (malonic and malic) are also converted to oxalate, finally yielding $K_2 [MoO(O_2)_2(ox)]$. <28> It appears that the presence of imidazole may enhance the catalytic ability of the system, at least in the case of aspartate.

While crystalline complexes have not been separated from the other systems studied here, some apparent mixtures have been obtained. Further refinement of their preparation procedures may yield pure complexes.

Once the x-ray structure analysis of the pure complexes is complete the biological activity of these compounds will be examined including antitumor activity. These compounds are also of interest as potential catalysts in the epoxidation of olefins.

One very important aspect of these complexes is their shelf-life. Many transition metal-peroxo complexes are quite unstable, with a shelf-life of only a few days or weeks. Our complexes, on the other hand, have shown little or no decomposition for up to a year. This stability will make further study of the complexes much easier.

References

1. Seigel, H. Metal Ions in Biological Systems vol. 6. Marcel Dekker. New York. 1983.
2. Chasteen, D.N. Structure and Bonding. (1983). 53. 107.
3. Sayers, D.L. and Eustace, R. The Documents in the Case. Avon Books. USA. 1968.
4. Venugopal, B. and Luckey, T.D. Metal Toxicity in Mammals-2. Plenum Press. New York. 1978.
5. Neilsen, F.H.; Myron, D.R.; Uthus E.O. Int. Symp. on Trace Element Metabolism in Man and Animals. M. Kirchgessner ed. Freising Germany. (1977). 244.
6. Cotton, F.A.; Wilkinson, G. Advanced Inorganic Chemistry: A Comprehensive Text 3rd ed. Wiley. New York. 1972.
7. Clark, R.J.H.; Brown, D. The Chemistry of Vanadium, Niobium and Tantalum. Pergammon Press. New York. 1975.
8. Rossotti, F.J.C.; Rossotti, H.S. Inorg. Nucl. Chem. (1956). 2 . 201.
9. Rossotti, F.J.C.; Rossotti, H.S. Acta. Chem. Scand. (1956). 10. 957.
10. Brito, F. Acta. Chem. Scand. (1967). 22. 1968.
11. Mulks, C.F.; Kirste, B.; von Willigen, H. J. Am. Chem. Soc. (1982). 104. 5906.
12. Patai, S. The Chemistry of Peroxides. Wiley. New York. 1983.
13. Djordjevic, C.; Craig, S.A.; Sinn, E. Inorg. Chem. (1985). 24. 1281.
14. Djordjevic, C.; Wampler, G.J. J. Inorg. Biochem. in press.
15. Quilitzsch, U.; Weighardt, K. Inorg. Chem. (1981). 20. 51.

16. Dean, G.A. Can. J. Chem. (1961). 39. 1174.
17. Chaudhuri, M.K.; Ghosh, S.K. Inorg. Chem. (1982). 21. 4020.
18. Djordjevic, C. Chem. Br. (1982). 18. 554.
19. Vuletic, C.; Djordjevic, C. J.C.S. Dalt. Trans. (1973) 1137.
20. Schwendt, P.; Joniakova, D. Polyhedron. (1984). 3. 287.
21. Funahashi, S.; Midorikawa, S.; Tanaka, M. Inorg. Chem. (1980). 19. 91.
22. Drew, R.E.; Einstein, F.W.B. Inorg. Chem. (1973). 12. 829.
23. Wieghardt, K. Inorg. Chem. (1978). 17. 57.
24. Djordjevic, C. Rev. Roum. Chim. (1977). 22. 601.
25. Djordjevic, C.; Vuletic, N. Inorg. Chem. (1980). 19. 3049.
26. Lehninger, A.L. Biochemistry. Worth. New York. 1982.
27. Steifel, E.I. Prog. Inorg. Chem. (1977). 22. 1.
28. Ochiai, E. Bioinorganic Chemistry: An Introduction. Allyn and Bacon. Boston. 1977.
29. Rollinson, C.L. The Chemistry of Chromium, Molybdenum and Tungsten Pergamon Press. New York. 1975.
30. Anke, M.; Grun, M.; Partsschefeld, M.; Groppel, B. Int. Symp. of Trace Element Metabolism in Man and Animals-3. Freising Germany. (1977). 230-233.
31. Mills, C.F.; Bremner, I.; El-Gallad, T.T.; Dalgarno, A.C.; Young, B.W. Int Symp. of Trace Element Metabolism in Man and Animals-3. Freising Ger. (1977). 150.
32. Hein, F.; Herzog, S. Handbook of Preparative Inorganic Chemistry vol. 2. Academic Press. New York. (1965). 1402.

33. Fischer, E.O. Inorg Syn. (1963). 7. 136.
34. Jolly, W.L. Inorg. Syn. (1968). 11. 116.
35. Cotton, F.A.; Wilkinson, G. Advanced Inorganic Chemistry 4th. ed. Wiley. New York. 1980.
36. Spence, J.T.; Lee, J.Y. Inorg. Chem. (1965). 4 385.
37. Baird, M.C. Prog. Inorg. Chem. (1968). 28.
38. Lucas, B.; Sandor, E. Acta. Cryst. (1963). 16. 854.
39. Cotton, F.A.; Morehouse, S.M.; Wood, J.S. Inorg. Chem. (1964). 3. 1603.
40. Conner, J.A.; Ebsworth, E.A.V. Adv. Inorg. Chem. and Radiochem. (1964). 6.
41. Richardson, E.J. J. L. Com. Met. (1960). 2. 360.
42. Stromberg, R. Acta. Chem. Scand. (1970). 24. 2024.
43. Djordjevic, C; Covert, K.J.; Sinn, E. Inorg. Chim. Acta. (1985). 101. L37.
44. Djordjevic, C. et. al. to be published.
45. Sundberg, C.; Martin, R. Chem. Rev. (1974). 74. 471.
46. Grimmett, M.R. Comprehensive Heterocyclic Chemistry. vol 5. part 4a.. Potts, K. ed. Pergamon Press. 1984.
47. Paquette, L.A. Principles of Modern Heterocyclic Chemistry. W.A. Benjamin Inc. New York. 1968.
48. Mohen, M.S.; Bancroft, D.; Abbott, E.H. Inorg. Chem. (1979). 18. 1527.
49. Freeman, H.C. Inorganic Biochemistry vol 1. Elsevier. New York. 1973. 121-166.
50. Akhtur, F.; Goodgame, D.M.L.; Goodgame, M.; Rayner Canhan, G.W.; Skrapski, A.C. Chem. Commun. (1968). 1389.
51. Freeman, H.C. Adv. Protein. Chem. (1967). 22. 293.
52. Kolks, G.; Frihart, C.R.; Coughlin, P.K.; Lippard, S.J

- Inorg. Chem. (1981). 20. 2933.
53. Davis, W.M.; Dewan, J.C.; Lippard, S.J. Inorg. Chem. (1981). 20. 2928.
54. Strandberg, R.; Lundberg, B.K.S. Acta. Chem. Scand. (1971). 25. 1767.
55. Mighell, A.D.; Santoro, A. Acta. Cryst. Sect. B. (1971). 27. 2089.
56. Antti, B.M.; Lundberg, B.K.S; Ingri, N. Chem. Commun. (1972). 712.
57. Lundberg, B.K.S. Acta. Chem. Scand. (1972). 26. 3977.
58. Lundberg, B.K.S. Acta. Chem. Scand. (1972). 26. 3902.
59. Anatolini, L.; Saladini, M.; Marcotrigano, G. Menabue, L.; Pellacini, G.C.; Inorg. Chem. (1982). 21. 2263.
60. Battaglia, L.P.; Corradi, A.B.; Antolini, L.; Marcotrigano, G.; Menabue, L.; Pellacani, G.C. J. Am. Chem. Soc. (1982). 104. 2407.
61. Seigel, H. Metal Ions in Biological Systems vol. 9. Marcel Dekker. New York. 1983.
62. McDonald, C.C.; Phillips, W.D. J.A.C.S. (1963). 85. 3736.
63. Delbeare, L.T.J.; Prout, C.K. Chem. Commun. (1971). 162.
64. Anatolini, L.; Battaglia, L.P.; Corradi, A.B.; Marcotrigiano, G.; Menabue, L.; Pellacani, G.C.; Saladini, M. Inorg. Chem. (1982). 21. 1391.
65. Suzuki, M.; Ueda, I.; Kanatomi, H.; Murase, I. Bull. Chem. Soc. Jpn. (1983). 56. 3421.
66. Glowack, T.; Wnek, I. Acta. Cryst. (1985). C41. 324.
67. Evans, D.J.; Kane-Maguire, L.A. Inorg. Chim. Acta. (1982). 62. 109.

68. Chacko, V.P.; LaMar, G.N. J.A.C.S. (1982). 104. 7002.
69. Goff, H.M.; Phillips, M.A. J.A.C.S. (1983). 105. 7567.
70. Shirazi, A.; Barbush, M.; Ghosh, S.; Dixon, D.W. Inorg. Chem. (1985). 24. 2495.
71. Boucher, H.A.; Lawrance, G.A.; Sargestar, A.M.; sangster, D.F. Inorg. Chem. (1983). 22. 3482.
72. Storm, C.B.; Freeman, C.M.; Butcher, R.J.; Turner, A.H.; Rowan, N.S.; Johnson, F.O.; Sinn, E. Inorg. Chem. (1983). 22. 678.
73. Brewer, G.; Sinn, E. Inorg. Chim. Acta. (1984). 87. L41.
74. Garrett, T.P.J.; Guss, J.M.; Freeman, H.C. Acta. Cryst. (1983). C39. 1027.
75. Hansen, A.P.; Goff, H.M. Inorg. Chem. (1984). 23. 4519.
76. Sandmark, C.; Brandin, C. Acta. Chim. Scand. (1967). 21. 993.
77. Dennis, A.M.; Howard, R.A.; Bear, J.L. Inorg. Chim. Acta. (1982). 66. L31.
78. Marzotto, A.; Kollowsky, H. Inorg. Chim. Acta. (1982). (1982). 67. 87.
79. Archer, S.J.; Auf der Hyde, T.P.E.; Foulds, G.A. Thornton, D.A. T. Met. Chem. (1982). 7. 59.
80. Bonsor, D.H.; Dean, B.R.; Wood, S.J. Can. J. Chem. (1976). 54. 2458.
81. Silverstein, R.M.; Bassler, G.C.; Morrill, T.C. Spectrophotometric Indentification of Organic Compounds. 4th ed. Wiley. New York. 1981.
82. Laitinen, H.A. Chemical Analysis. McGraw-Hill. New York. 1960.
83. Flashka, H.A.; Barnard, A.J.; Sturrock, P.E. Quantitative Analytical Chemistry vol. II. Barnes and Noble. New York. 1969.
84. Vogel, A.I. A Textbook on Quantitative Inorganic

Analysis 3rd ed.. Longmans. London. 1966.

Vita

JENNIFER LISA GUNDERSEN

Born in Point Pleasant, New Jersey, 13 April, 1963.
Graduated from Saint Rose High School in Belmar, New
Jersey, June 1981, B.S. College of William and Mary in
Virginia, May 1985. M.A. candidate, College of William
and Mary in Virginia, 1985-86.